



Western Michigan University
ScholarWorks at WMU

Dissertations

Graduate College

8-2018

Screen Printed Moisture Sensor On Barrier Coated SBS Board: The Characterizations of the Hemicellulose-Based Biofilms and Their Applications for Smart Packaging

Ruoxi Ma

Western Michigan University, rachelmaruoxi@gmail.com

Follow this and additional works at: <https://scholarworks.wmich.edu/dissertations>

 Part of the Chemical Engineering Commons

Recommended Citation

Ma, Ruoxi, "Screen Printed Moisture Sensor On Barrier Coated SBS Board: The Characterizations of the Hemicellulose-Based Biofilms and Their Applications for Smart Packaging" (2018). *Dissertations*. 3327. <https://scholarworks.wmich.edu/dissertations/3327>

This Dissertation-Open Access is brought to you for free and open access by the Graduate College at ScholarWorks at WMU. It has been accepted for inclusion in Dissertations by an authorized administrator of ScholarWorks at WMU. For more information, please contact wmu-scholarworks@wmich.edu.



SCREEN PRINTED MOISTURE SENSOR ON BARRIER COATED
SBS BOARD: THE CHARACTERIZATIONS OF THE
HEMICELLULOSE-BASED BIOFILMS AND THEIR
APPLICATIONS FOR SMART PACKAGING

by

Ruoxi Ma

A dissertation submitted to Graduate College in
partial fulfillment of the requirements for
the degree of Doctor of Philosophy
Chemical and Paper Engineering
Western Michigan University
August 2018

Doctoral Committee:

Alexandra Pekarovicova, Ph.D.,
Chair Paul D. Fleming III, Ph.D.
Veronika Husovska, Ph.D.

Copyright
by Ruoxi Ma
2018

SCREEN PRINTED MOISTURE SENSOR ON BARRIER COATED SBS BOARD: THE CHARACTERIZATIONS OF THE HEMICELLULOSE-BASED BIOFILMS AND THEIR APPLICATIONS FOR SMART PACKAGING

Ruoxi Ma, Ph.D.

Western Michigan University, 2018

Fiber-based packaging materials have many advantages over their petroleum-based plastic competitors, such as sustainability, recyclability and stiffness/weight ratio. However, the poor barrier properties and sensitivity towards moisture are the main challenges for their extended use. Therefore, there has been a need to provide a biodegradable and biocompatible biopolymer packaging material with improved barrier properties for food and pharmaceutical packaging. Also, the moisture loss/gain problem causes a lot of waste every year. Therefore, there is a need of better tracking and sensing methods attached to the package in order to control the moisture level along the supply chain. To accomplish these goals, three studies have been designed: a) The preparation of the hemicellulose-based films and the characterization of surface, strength and printability properties. b) The barrier properties of the hemicellulose-based biofilm were characterized with moisture vapor transmission rate. The hydrophobic property and moisture barrier property of hemicellulose-based biopolymer were improved by crosslinking with citric acid and further characterized by moisture vapor transmission rate (MVTR). c) The barrier coating was formulated and applied to the back side of solid bleached sulphate (SBS) board and was screen printed with a moisture sensor. The moisture sensor was characterized by its impedance with various relative humidity ranges. The findings provide the possibility of combining the hemicellulose-based biodegradable barrier coatings with printed moisture sensors in order to boost their capabilities in smart packaging applications.

ACKNOWLEDGEMENTS

I would like to thank my advisor Dr. Sasha Pekarovicova for all her contributions to this work, and my education. Who, without her dedicated assistance and guidance this work would have not been possible. I also give thanks to Dr. Dan Fleming, Dr. Veronika Husovska for all their valuable contributions and insights into this research.

I would also give my thanks to Paper Technology Foundation at Western Michigan University, for their generous support both financial and technical. I sincerely appreciate all the assistance provided by Mr. Matthew Stoops for his assistance in helping me to understand and use the testing equipment necessary for completion of this work.

I would like to thank my family, friends, and loved ones for all their encouragement and support, without which, this work would have not been possible. With a special thanks to my parents for all they have done for me both for my education and personal life, without which, none of this would be possible.

Ruoxi Ma

TABLE OF CONTENTS

ACKNOWLEDGEMENTS	ii
LIST OF TABLES	vi
LIST OF FIGURES	viii
NOMENCLATURE AND ABBREVIATIONS	xi
CHAPTER 1	1
INTRODUCTION	1
1.1 Flexible Packaging and Biodegradable Polymers	2
1.2 Barrier Coatings	3
1.3 Printed Electronics	4
1.4 Printing Method	8
1.5 Statement of Problem	11
1.6 Motivations for Study	12
1.7 Objectives of Research	13
CHAPTER 2	15
LITERATURE REVIEW	15
2.1 Introduction	15
2.2 Hemicellulose and Its Application	15
2.3 Nanofibrillated Cellulose	17
2.4 Barrier Coatings	21
2.5 Crosslinking of Polysaccharides and MVTR	24
2.6 Inks and Substrates for Printed Electronics	27
2.7 Substrate Wetting and Ink Spreading	30
2.8 Smart Packaging and Moisture Sensor	37
CHAPTER 3	43
PREPARATION AND CHARACTERIZATION OF HEMICELLULOSE-BASED FILMS	43
3.1 Abstract	43
3.2 Introduction	44
3.3 Experimental	50

Table of Contents - continued

3.4 Results and Discussion	55
3.5 Conclusions	70
CHAPTER 4	71
BIOPOLYMER FILMS FROM GLUCOMANNAN: THE EFFECTS OF CITRIC ACID CROSSLINKING ON BARRIER PROPERTIES	71
4.1 Abstract	71
4.2 Introduction	71
4.3 Experimental	76
4.4 Results and Discussion	82
4.4.1 Caliper	82
4.4.2 Moisture Vapor Transmission Rate (MVTR)	83
4.4.3 Tensile Properties	85
4.4.4 Surface Energy	86
4.4.5 Solubility	87
4.5 Conclusions	88
CHAPTER 5	89
SCREEN PRINTED MOISTURE SENSOR ON HEMICELLULOSE-BASED BARRIER COATED SBS BOARD	89
5.1 Abstract	89
5.2 Introduction	90
5.3 Experimental	97
5.3.1 Materials	97
5.3.2 Coating Formulation	98
5.3.3 Calendering and Conditioning of Samples	99
5.3.4 Sensor Printing	99
5.3.5 Sensor Testing	100
5.4 Result and Discussion	102
5.4.1 Barrier Properties Analysis	102

Table of Contents - continued

5.4.2 Humidity Sensor Response Analysis	103
5.5 Conclusion	109
CHAPTER 6	111
CONCLUSION AND FUTURE WORK	111
6.1 Contribution to General Science	113
6.2 Contribution to Development of Practical Applications	113
REFERENCES	115
LIST OF PUBLICATIONS	129

LIST OF TABLES

1. Materials Commonly Used as Substrates in PE [57].	27
2. Hemicelluloses and Their Sources [86].	45
3. Formulation of Biofilms.	51
4. The Factors and Levels in ANOVA Analysis for the Film Formulations.	56
5. ANOVA for Tensile Strength Versus Nano-fibrillated Cellulose (NFC).	56
6. The ANOVA Table for Tensile Strength versus Sorbitol.	57
7. The ANOVA Table for Tensile Strength versus Glucomannan.	58
8. Surface Tension of Liquid Phases with Values of Dispersion and Polar Components Used in Owens-Wendt Calculations.	67
9. Owens-Wendt Method of Estimating Surface Free Energy Values of Hemicellulose Film #4 (DI- distilled water, MI- methylene iodide).	67
10. Owens-Wendt Method of Estimating Surface Free Energy Values of PET Film (DI- distilled water, MI- methylene iodide).	68
11. Owens-Wendt Method of Estimating Surface Energy Values of Kraft Paper (DI- distilled water, MI- methylene iodide).	68
12. The Crosslinking Film Formulations.	78
13. MVTR Permeability Properties of Polypropylene and Other Plastics Films [138].	80

List of Tables - continued

14. The Caliper of Hemicellulose-based Films.....	83
15. The Tensile Properties of the Hemicellulose-based Films.....	86
16. The Surface Energy Estimation of the Film Surfaces.....	87
17. The Solubility Values of the Film Series.	87
18. The Crosslinking Barrier Coating Formulation.	98
19. Barrier Properties of the Hemicellulose-based Coated Board.	103

LIST OF FIGURES

1. The Illustration of Additive and Subtractive Printing Process [14].	6
2. Fine Line Screen Printing [17]. (a) 8 μ m Width Ag Nanoparticle Ink Pattern and Screen Mask. (b) High Aspect Ratio: 19 μ m Height, Cu Particle Ink Patterning with L/S=20/20 μ m.	9
3. The Parameters in Screen Printing [17].	10
4. (a) Micro-composites: Pigment Particle Size: Length (μ m) Width (μ m) Thickness (μ m) (b) Nano-composites: Pigment Particle Size: Length (μ m) Width (μ m) Thickness (μ m) [44].	23
5. Transparency of Nanofiber Paper and PET Films [61]. Total Light Transmittance During Heating at 150 °C for 120 min (Solid Square: Nanofiber Paper; Solid Circles: PET) and Haze During Heating at 150 °C for 120 min (Square: Nanofiber Paper; Circles: PET).	30
6. Contact Angle of Liquid on a Substrate [62].	33
7. Contact Angle and Wetting Rate [61].	34
8. The Calculation of the Shape Factor β .	35
9. An Example of Zisman Plot [65].	37
10. Schematic of the Layout of a Planar IDT moisture sensor [75].	40
11. A Cross Section of the Moisture Sensor, with the Moisture Sensitive Substrate, the Dielectric Layer and the Conductive Sensor Layer [76].	40

List of Figures - continued

12. The Main Components of Hemicelluloses [92].	46
13. Commonly Used Plasticizers for the Hemicellulose-based Films [93].	50
14. Glucomannan Composed of β -D-Glucopyranose and β -D-Mannopyranose Units Linked by 1 \rightarrow 4 β -D- Glycosidic Bonds (Second Glucopyranose Unit is Esterified) [98].	51
15. The Tensile Strength of the Hemicellulose Based Films, Paper and PET Film.	59
16. The Elongation of the Hemicellulose-based Films, Paper and PET Film.	60
17. The Bursting Strength of the Hemicellulose-based Films, Paper, and PET Film.	62
18. The Air Permeability of Hemicellulose-Based Films, Kraft Paper and PET Film.	64
19. The Roughness of Hemicellulose-based Films, Kraft Paper and PET Film.	65
20. The Caliper of Hemicellulose-based Films, Kraft Paper and PET Film.	66
21. Optical Density of Solid Patch Printed on Glucomannan Films, Paper and PET Film.	69
22. Mechanism for Covalent Crosslinking [113].	73
23. The Thwing-Albert EZ-Cup and Tested Films [138].	81
24. The Moisture Vapor Transmission Rate for the Hemicellulose-based Films.	84

List of Figures - continued

25. The Design Interdigitated Electrode (a) and Its Detailed Structure (b) [170].	95
26. The Experiment Setup for the IDE Humidity Sensor Printing and Characterizations.	101
27. The Stepwise Change of the Relative Humidity in the Test Chamber.	104
28. Capacitance vs. RH Plot of Sensor Printed on Uncoated SBS Board.	105
29. Capacitance vs. RH Plot of Sensor Printed on Coated SBS Board.	106
30. Resistance vs. RH Plot of Sensor Printed on Coated SBS Board.	107
31. Resistance vs. RH Plot of Sensor Printed on Uncoated SBS Board.	108

NOMENCLATURE AND ABBREVIATIONS

CA	Citric acid
CNFs	Cellulose nanofibers
DI	Deionized ultra-filtered water
DoE	Design of Experiment
HE	Hexadecane
IDE	Interdigitated electrodes
IR	Infrared
LCR	Inductance capacitance resistance
LDPE-	Low-density polyethylene
MFC	Microfibrillated cellulose
MI	Methylene iodide
MVP	Moisture vapor permeability
MVTR	Moisture vapor transmission rate
NFC	Nanofibrillated cellulose
PE	Printed electronics
PET	Polyethylene terephthalate
PET	Polyethylene terephthalate
SBS	Solid bleached sulfate

CHAPTER 1

INTRODUCTION

The purpose of this part is to provide readers with basic information pertaining to biodegradable polymers, barrier coatings and printing electronics. What hemicellulose and nanofibrillated cellulose (NFC) are, as well as the basic motivations for use of hemicellulose-based coated SBS board in printing electronics for moisture sensors and their possible applications. Current applications of polysaccharides as biodegradable films, as well as some current limiting factors pertaining to the food and pharmaceutical packaging applications and the methods to improve their barrier properties against moisture and oxygen are reviewed. Ink and printing methods used in printed electronics are discussed, with a focus on the benefits of optimizing performance of printed metallic inks onto a biodegradable substrate. Lastly, the current research and applications on the use of biodegradable barrier coatings for the creation of printed electronics and the working principles of printed moisture sensors are discussed.

1.1 Flexible Packaging and Biodegradable Polymers

Flexible PET (Polyethylene Terephthalate) or LDPE (Low-density Polyethylene) films, known as the plastic films, are currently the main substrates for food and pharmaceutical packaging. Plastics have been the dominant packaging materials because of their balanced properties in relation to other thermoplastic polymers. However, the common plastic films can't be dissolved or degraded, which causes serious pollution and sustainability issues. For example, if the plastic is incinerated, it increases carbon emissions and dioxin; if it is placed in a landfill, it becomes a carbon sink.

Generally, biocomposites are totally biodegradable and are found to fully disintegrate in ideal conditions [1]. Biodegradation is governed by different factors including polymer characteristics, type of organism, and the nature of pretreatment [2]. Various microorganisms such as bacteria and fungi are responsible for the degradation of both natural and synthetic polymers [3]. Compared to conventional polymers, the biopolymers based on cellulose, hemicellulose and nanofibrillated cellulose (NFC) are fully biodegradable in a wide variety of environmental conditions [4]. Cellulosic fibers have traditionally been used in packaging for a wide range of

food categories such as dry, frozen or liquid foods and beverages [5].

1.2 Barrier Coatings

Paper coatings are applied as an aqueous suspension of a pigment and binder in soluble or particulate form. The aqueous phase is then dried using hot air and IR dryers and the structure is formed. The first (gloss) critical concentration is reached when the pigment particles are brought into contact with one another, and a matrix is formed [6]. The fluid phase is however still mobile, and the structure may shrink until the second (opacity) critical concentration is reached, after which the binder has sometimes formed a film and then coating no longer exists as separate particles [7].

Solid bleached sulfate (SBS) paperboards manufactured from cellulosic wood fibers fulfill many of the requirements of primary recycling since cellulose is biodegradable. SBS is a premium paperboard grade that is produced from fully bleached virgin kraft pulp (sulfate process) fiber.

The major markets for SBS are folding cartons such as milk and juice cartons and recyclable food service products such as paper cups, plates and food containers [8].

Packaging made from SBS paperboards has therefore been extensively used to contain perishable

products. Unfortunately, due to the high gas permeability and hydrophilicity of cellulosic fibers, perishable and liquid products cannot be contained in simple paperboard containers. In order to overcome these difficulties, paperboard packages are commonly extrusion coated off-line with unsustainable petroleum based products [9], such as polyethylene, polypropylene and polyethylene terephthalate, etc. to improve barriers against water, water vapor and gases [10]. Above all, the recycling of petroleum based products coated on SBS paperboard is extremely difficult. In addition, the mechanical properties of baseboard are affected during the extrusion process as temperature can reach in excess of 300 °C [11], above the glass transition temperature T_g of cellulose, hemicellulose and lignin.

Thus, the paper manufacturers' desire to produce paperboard for barrier applications on machine in a single run, and consumer pressure to reduce the amount of non-recyclable petroleum based products have created a need for research in dispersion coatings with biodegradable materials.

1.3 Printed Electronics

Printed Electronics (PE) has been introduced to not only the electronics industry, but also to all kinds of electronically controlled machines and device manufacturer in the past few decades. PE

are electrically functional devices or components (e.g. Electrodes) formed by an imaging process. It has emerged as one of the key technologies to combine printing process with electronics manufacturing. Compared to the traditional additive electronics manufacturing, PE products are thin, flexible, wearable, lightweight, of varying sizes, ultra-cost-effective, and environmentally friendly.

Printed Electronics may generally be categorized as either being additive or subtractive.

Subtractive PE is most often associated with conventional electronic production process such as photolithography. Photolithography is a process used in both the fabrication of conventional electronics and by the printing industries for the imaging of plates used to create an image carrier

[12]. So, it is a process technology not foreign to printers. In its use for the creation of conventional electronics systems, a layer of photoresist (a polymer that is altered by UV exposure by becoming more basic, acidic, or neutral) is deposited evenly onto a substrate, covered with a mask bearing the desired pattern to be created. The photoresist layer is then exposed to a dosage of UV light that is specific to its particular formulation and layer thickness.

Dependent on the type of photoresist used, the type of chemical bath to wash away the unreacted

areas is chosen, allowing reacted areas to remain [13]. The use of environmentally unfriendly chemicals is inherent in these processes, which produce large amounts of waste. In addition to generating much waste, conventional PE, being a subtractive process, requires multiple costly and time consuming processing steps.

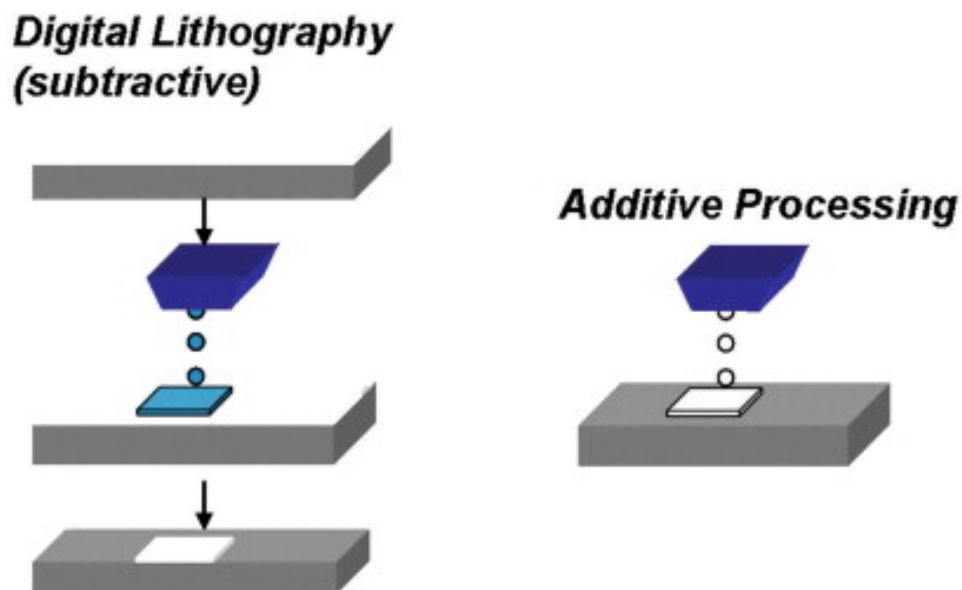


Figure 1 The Illustration of Additive and Subtractive Printing Process [14].

Additive PE most often refers to the production of electronic components/devices using additive deposition processing, such as screen printing of functional inks. Additive PE is not a new concept; in fact, it has been around since the early 1950s. However, due to recent advancements in process and material technologies along with the desire and need to create new form factors,

PE has gained much interest. Additive PE provide the advantages of enabling more environmentally friendly, lower cost production, and the ability to create new form factors (i.e. wearable sensors) electronics [15].

Printing electronics is a more environmentally friendly [16] alternative to conventional methods for the creation of PE devices and components because there are more opportunities for reclamation of materials. Printing electronics may be accomplished with the use of (additive) printing methods, which include: screen, inkjet, gravure, flexography, and offset lithographic printing processes. The processes involved in the use of conventional graphic printing, are the same ones used in the processes employed to print electronics, the only difference is that of the materials used for the creation of the inks. This is why printing electronics is often referred to as functional printing. For example, screen-printing uses thick films of mixed polymer pastes (inks) that may either contain metallic particles or flakes for functional printing, or pigments and dyes for graphic printing. The screen-printing process is very simple but yields high material costs due to the inherent thick ink-film produced and subsequent larger ink volumes used. As mentioned above, an advantage of PE is its environmental friendliness, which is resultant of the ability to

reclaim a large portion of the high value materials used. The ability to reclaim a high portion of these materials is economically favorable by helping to lower waste. Another economic benefit is that some inks can be reclaimed. For example, precious metals used for conductive inks, such as silver or gold can be reclaimed and re-used. As the world demand of electronics continues to grow, and resources continue to dwindle, the use of PE will likely be increasingly used for this increasingly important benefit.

The choice of printing methods is critical before launching research projects. There is no single selection for one application. There are certain suitable matchings between inks and printed electronics. A substrate may play a role in this choice. Not only the viscosity/surface tension of the ink but the device structure and whether the device is thin or narrow will affect the pattern quality obtained.

1.4 Printing Method

Screen printing is one of the most common printing methods and has been used for many years in electronics manufacturing. The most distinct feature of screen printing compared with other printing methods is the high aspect ratio of printed objects. The usual thickness of a screen-

printed image is in the range of several tens of microns, but, especially when a thick screen mesh is used, the thickness can exceed 100 μm with a single pass of printing, which cannot be obtained by any other printing method. For other methods, such as inkjet or flexographic printing, the typical thickness is less than 5 μm [17]. Figure 2 shows a high-aspect-ratio screen-printed line example.

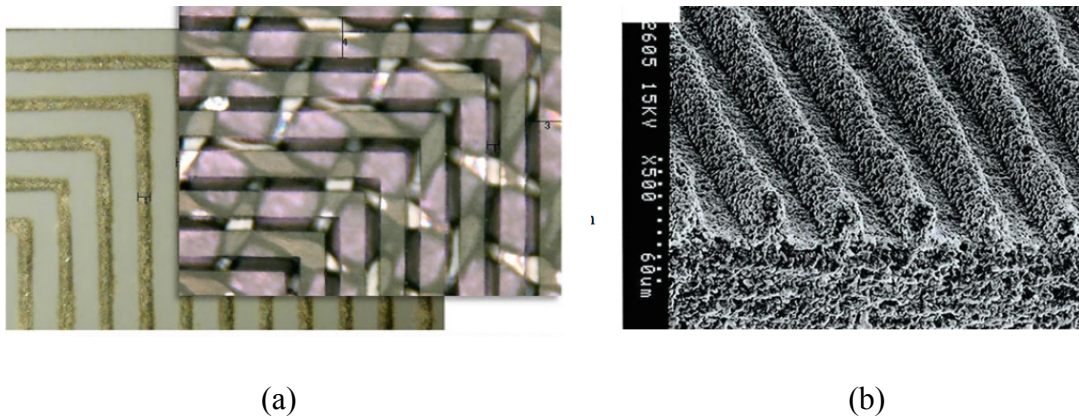


Figure 2 Fine Line Screen Printing [17]. (a) 8 μm Width Ag Nanoparticle Ink Pattern and Screen Mask. (b) High Aspect Ratio: 19 μm Height, Cu Particle Ink Patterning with L/S=20/20 μm .

In screen printing, as schematically shown in the Figure 3, printing is performed at a low printing pressure using a screen mesh with a designed pattern of uniform thickness. A flexible metal squeegee or rubber squeegee is used for squeezing paste through the mesh. A polymer mesh, such as polyamide/polyester, or a stainless steel mesh can be used. A mesh pattern is formed by photolithography of an emulsion on the mesh. Instead of a mesh screen with an emulsion pattern,

a metal screen can also be used.

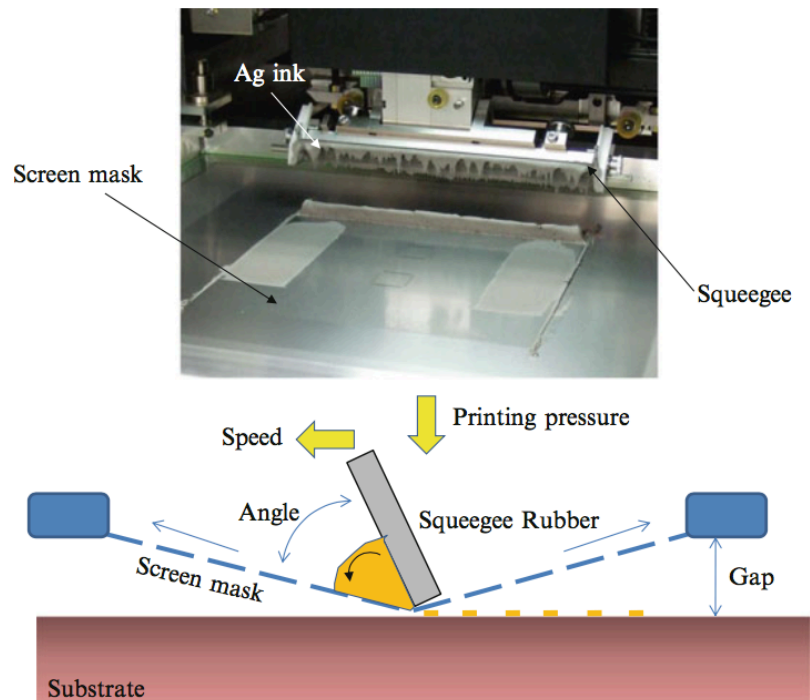


Figure 3 The Parameters in Screen Printing [17].

1.5 Statement of Problem

Barrier coated packaging is an extremely large and important area of interest to manufacturers, retailers and consumers. It is expected to grow rapidly as industry expands its offerings of specialty foods, functional foods, extended shelf life products, convenience foods and serving ware such as paper cups and plates. Consumers are demanding longer shelf life, safety and added value packaged products. On one hand, the environmental sustainability requires a biodegradable and biocompatible packaging materials to serve as sustainable barrier systems. The need to reduce the amount of non-recyclable and unsustainable barrier materials such as petroleum-based products is growing. On the other hand, the smart packaging that combines printed electronics with flexible, disposable and porous substrate has been increasing when compared to polymer-based printed electronic devices. There is an increasing need to develop low cost, disposable, light weight and environmental friendly humidity sensors to better track moisture gain/loss of packaging along the transportation and storage, where extremely high/low humidity conditions usually cause the material failure or fatigue, hence damage the product that the barrier packaging serves to protect.

1.6 Motivations for Study

Flexible petroleum-based plastic films have been the dominant substrates for food and pharmaceutical packaging for over several decades. This is due to their good strength, barrier and optical properties. However, the common plastics can't be dissolved or degraded, which causes serious pollution and sustainability issues.

Therefore, global sustainability calls for more biodegradable and biocompatible materials.

Natural polymers, such as polysaccharides, are ideal starting materials for these kinds of composites due to their biodegradability, biocompatibility, non-toxicity and renewability.

Hemicelluloses are heteropolysaccharides that are mostly dissolved in the process of making pulps and paper from wood. By their chemical nature, they are hydrophilic, and can offer barrier against fats and oils and oxygen. However, the hydrophilicity of hemicelluloses has limited their application in packaging materials. Therefore, this study aims to improve the moisture barrier property of hemicellulose-based biopolymers by crosslinking.

In the past decade hybrid materials for highly stretchable, conductive electrodes have received tremendous attention in the fields of emerging wearable electronic and sensing devices.

According to the insurance business, a lot of waste occurs every year due to the moisture loss/gain or water leakage damage. The current trend in transportation and distribution is to target systems that provide higher visibility and tracking convenience, thus better control over the supply chain. Printed electronics provide a portable, inexpensive and flexible solution to better track the moisture level along the transportation and storage of the moisture sensitive product such as cereals and potato chips. This study aims to combine the biodegradable barrier coated SBS board with a printed moisture sensor to provide a flexible, stretchable and disposable device for smart packaging application.

1.7 Objectives of Research

The objective of this research is to advance the knowledge of the material properties of the hemicellulose-based biofilms, their interactions with conductive inks and printability towards achieving more applicable PE devices. To accomplish these objectives, this dissertation research will be organized and advanced into three projects.

In the first project, the formulations of hemicellulose-based printable films were performed through a full factorial design of experiments (DoE). The effects of various types and amounts of

nanofibrillated cellulose and various blending methods on the properties of the films were studied by using the DoE method. The films were characterized by their printability, strength (tensile, bursting and elongation) and surface properties (smoothness and surface energy).

In the second project, the hydrophobicity of the hemicellulose-based films was improved by crosslinking the free hydroxyl groups with citric acid. The barrier properties of hemicellulose-based biopolymers against moisture and air were characterized by the air permeability, moisture vapor transmission rate (MVTR) and insoluble matter.

In the third project, a barrier coating formulation was developed based on the best formulation of the hemicellulose-based crosslinked film. The coatings were applied to solid bleached sulphate (SBS) paperboards and then calendered to 3 μm PPS roughness. A humidity sensor with interdigitated electrodes was printed onto the barrier-coated SBS board with silver conductive ink using the screen printing method. The printed sensor was calibrated, followed by characterizations of the sensor's impedance change with each moisture level ranging from RH 20% to 80%. The breakthrough time was observed for each level of RH by measuring impedance using an LCR meter.

CHAPTER 2

LITERATURE REVIEW

2.1 Introduction

The purpose of this chapter is to provide readers with basic information pertaining to hemicellulose and nanofibrillated cellulose. What they are, as well as the current applications and their limitations to be used as packaging materials. Printed electronics, smart packaging and printed sensors are discussed, with a focus on barrier coatings and the characterizations of barrier properties, as well as some current limiting factors pertaining to the implementation of printing for the creation of functional devices.

2.2 Hemicellulose and Its Application

The petroleum-based packaging waste does not find its way only to landfills but also into seas, forests, and municipal landscapes. It degrades very slowly and pollutes the surrounding environment and is an extremely large hurdle all over the world. The small plastic particle waste (1-20 mm) is often dominant in the land areas next to the sea. These particles may place marine organisms at high risk due to possible ingestion [18]. Hence the appropriate legislation and

attitude changes are needed to implement and promote the research, availability, and the production of biodegradable and biobased materials. There is definitely an opportunity for the renewable natural fibers to be utilized as biomaterials. Thus, biopolymer composites are undoubtedly emerging [19].

Water soluble hemicelluloses can be obtained in large scale from side streams in mechanical pulping [20] or from pressurized hot-water extraction of wood [21]. Glucomannan extracted from konjac root is hydrophilic but it can be easily altered to more hydrophobic by grafting with non-polar groups [22] or by cross-linking chemically or enzymatically [23]. Amphiphilic glucomannan derivatives have been made using fatty acids, cationic groups or hydrophobic tails of polydimethylsiloxane [24]. In order to make pure films of glucomannan, fairly high plasticizer content is required. The added glycerol in micro-fibrillated cellulose (MFC)-glucomannan films decreases stiffness and strength but increases the elongation at break [25]. The incorporation of nanofibrillated cellulose (NFC) into pullulan films improves their mechanical properties. The addition of glycerol into these NFC-pullulan films enhances the flexibility and homogeneity of the films and also increases the Young's modulus and tensile strength even up to 800% [26].

In food packaging, several features can be tailored: for instance, mechanical and optical properties, gas permeability and barrier properties, convenience in use, biodegradability, and the green image. Hemicelluloses are known to have excellent oxygen barrier properties [27] and NFC is known to have excellent mechanical properties [28]. Hence, even with the added hydrophobic functionality within glucomannan-based substrates, they can be well-established onto the NFC network due to their chemical similarities. In this work, we aimed to enhance the mechanical strength as well as barrier properties with films made of glucomannan within the nanofibrillated cellulose (NFC) network. Moreover, the hydrophobicity of glucomannan-based films and coatings are improved with crosslinking by introducing citric acid.

2.3 Nanofibrillated Cellulose

Nanofibrillated cellulose (NFC) is one of the most interesting renewable nanomaterials obtainable from nature after processing. In addition to the obvious environmental reasons, the renewability, nontoxicity, and availability of cellulose, the growing interest for this material is due to its extraordinarily high specific strength, thermal stability, hydrophilicity, and broad capacity for chemical modification. Recently, the development in cellulosic fibrillation methods

has facilitated the production of nanoscaled NFC from cellulosic sources, such as wood and crops, with reasonable low energy consumption [29]. The width of the nanofibrils depends on the production method but is typically around 5-20 nm. The length of the fibrils is more challenging to determine but may exceed 5 μm , and thus, the aspect ratio of NFC can be more than 250. The high aspect ratio is advantageous and contributes to the high strength of network structures and composite materials prepared from NFC.

There is a great demand for flexible, strong, transparent, thermally stable films with excellent barrier properties for various packaging applications, such as food, medicine, and electronics. Especially, the gas barrier properties are important since even a very small amount causes most products to deteriorate. Petroleum-derived polymers have been extensively used due to their simple processing, low manufacturing costs, and excellent barrier properties. However, the increased environmental consciousness has promoted the utilization of biopolymers. Starch and regenerated cellulose films, such as cellophane, have been explored, but their strength properties are not always sufficient. Thus, they are traditionally mixed with synthetic ones or chemically modified [30] to improve their properties. The strong interaction between cellulose nanofibrils

during drying can be utilized to prepare NFC films [31]. The inherent strength of the cellulose crystals combined with the strength of interactions between the fibrils leads to the formation of very strong films based on NFC. NFC films also show excellent oxygen barrier properties in dry conditions. For a comprehensive review on the potential of NFC as a barrier material, the reader is referred to the recent review by Lavoine et al [32]. However, most practical applications demand that the film can stand at least 50% relative humidity. Only a few attempts have been made to enhance the barrier properties of NFC at elevated humidity. Spence et al. [33] found that lignin present in the NFC actually increased the water vapor transmission through the film, although the opposite was expected. This was concluded to be due to the increased permeability of the film. Similarly, acetylation of cellulose nanofibrils prior to film formation enhances the barrier properties only at very low degrees of substitution and had a deteriorating effect at higher levels of substitution [34]. Nanocomposite films containing nano-clay and NFC were found to retain good oxygen barrier properties even at high humidity [35]. Although the barrier properties of NFC films have gained much attention lately, the films' resistance to solvent has not been explored earlier.

NFC has been used for packaging applications for its good mechanical properties and low gas permeability rates. Entangled networks with inter-fibrillary hydrogen bonding of nanofibers are known to improve mechanical properties. However, NFC has its drawbacks. It is hygroscopic and the mechanical properties are weakening upon wetting. Presumption is that NFC has good affinity to hydrophilic polymers, but not to hydrophobic polymers. Regardless, Okuba et al. demonstrated that MFC reinforced a polylactic acid–bamboo fiber matrix so that bending strength and fracture toughness improved and also crack growth was prevented [36]. To overcome the challenge of weak water repellence, the hydrophobicity of NFC was improved with silylation. The silylated material combined both hydrophobicity and oleophilicity and could selectively remove oil at the surface of water. At the oil-water interface, the nanofibrillated cellulose was present as single dispersed fibrils or as a network [37]. The hydrophobicity of the fiber surface of NFC was enhanced by esterification with acetyl chlorides. A water dispersion of NFC was solvent-exchanged with acetone and then further with toluene [38]. NFC was incorporated into a matrix of acrylic polymer latex up to 15 wt% ratio, which led to major enhancement in the tensile modulus of the nanocomposite film [39]. The vulnerability of NFC

composites towards the solvent has also been studied: NFC films have the ability to resist polar and nonpolar solvents such as methanol and dimethylacetamide [40].

2.4 Barrier Coatings

Barrier composite coatings that provide water, water vapor and gas resistance through the paperboard package have been widely used in food packaging [41]. Barrier coated packaging is now more focused towards extending shelf life, minimizing microbial attack and ensuring food safety through control of the environment within the packaging. The packaging system is composed of substrates, coatings, barrier fluids, inks and varnishes. In addition, there are the contents of the packaging system that may be solid, liquid or gaseous, or mixtures of these components.

SBS baseboard is a complex material and is mainly composed of wood fibers (cellulose and hemicellulose), fillers (clays, carbonates, etc.), and various additives (sizing agents, retention aids, etc.) [42]. SBS properties depend on the fiber types and extent of fiber-fiber bonding, as well as on the network structure. The cellulosic fibers are a key constituent of any board-based

packaging and provide desired structural rigidity to the package. Unfortunately, due to the high water affinity, water vapor and gas permeability of cellulosic fibers, paperboards are commonly extrusion coated off-line with unsustainable petroleum based polymer barriers such as waxes, ethylenecoviny alcohol and plastics (polyethylene, polypropylene and polyethylene terephthalate, etc.) [43]. Above all, the recycling and repulpability of these polymers and plastics coated paperboards are extremely difficult.

Packaging products made from cellulosic materials are increasingly being modified and improved not only for barrier resistance but also for appearance and printability. The following strategies can be used to improve barrier performance (1) improve the quality of the barrier coating layer by reducing the defects and/or (2) adopt a multilayer coating structure and decouple the defects. These strategies were used by developing a nanostructured co-polymerized coating using HSFE (High Shape Factor Engineered) clays that reduce permeation via a tortuous path of pores within the coatings [44], as shown in Figure 4.

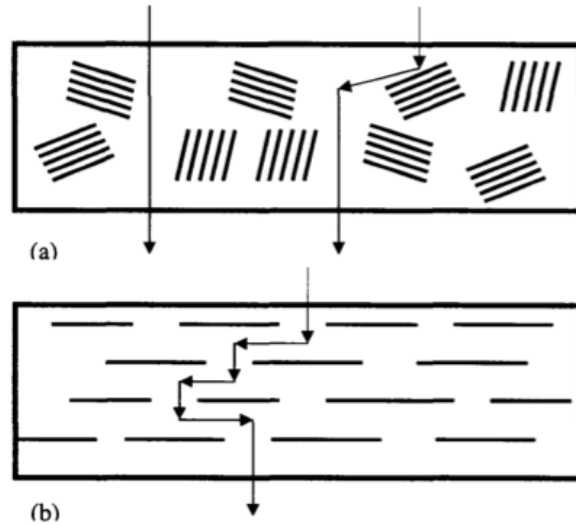


Figure 4 (a) Micro-composites: Pigment Particle Size: Length (μm) Width (μm) Thickness (μm)
 (b) Nano-composites: Pigment Particle Size: Length (μm) Width (μm) Thickness (μm) [44].

Nanocomposites [45] are a new class of materials that are particle filled polymers for which at least one dimension of the dispersed particles is in the nanometer range. We can distinguish three types of nanocomposites, depending upon how many dimensions of the dispersed particles are in the nanometer range. The first type is isodimensional nanoparticles, such as spherical silica nanoparticles, which are in the order of the nanometers in all the dimensions. The second type, whiskers or nanotubes such as cellulose whiskers [46] or carbon nanotubes [47], have two dimensions in the nanometer range and the third is larger forming an elongated structure. The third type, sheet like fillers or pigments such as HSFE clays [48], has only one dimension in thickness in nanometer range.

2.5 Crosslinking of Polysaccharides and MVTR

Usually films based on single biopolymers are highly sensitive to environmental conditions and generally possess low mechanical resistance [49]. Films can be produced by chemical cross-linking and physical blending. Polymer blending is an effective approach to endow new material with desired properties. Physically blending biopolymers and synthetic polymers to achieve desired features has received increasing attention in recent years.

Hemicellulose has received increasing interest especially in the last few decades for the production of biodegradable films and coatings [50]. However, free-standing hemicellulose cannot form a continuous film, and several efforts [51] have been made to overcome this drawback. One method is to add plasticizer into hemicellulose to enhance its film performance. However, plasticizers can increase the elasticity of the film, and also lead to an increase in hydrophilicity. As a result, researchers have shifted to examining the films of hemicellulose blends with other polymers [52]; as an example can be attempt to add lignin into xylan isolated from cotton stalks to produce a film for food packaging applications. Cellulose nanofibers

(CNFs) were found to be a good nano-reinforcement to improve the mechanical properties of xylan films [53]. At a CNF content of 20 wt%, the tensile stress and Young's modulus of the composite films increased up to 39.5 and 3404 MPa, respectively. Strong interactions could be formed between CNFs and xylan.

Glucomannan as the main component of hemicellulose, has an abundance of hydroxyl groups distributed along the backbone and side chains, and is thus an ideal candidate for the formation of hydrogen bonds when blending with citric acid. Citric acid (CA) is an inexpensive, non-toxic food additive, which has been used as a cross-linking agent to improve the performance of starch [54], cellulose [55], and PVA/starch [56] films. No information has been reported using CA as a plasticizer or cross-linking agent in glucomannan/NFC composite films to enhance the mechanical and barrier properties. This work aims to investigate the glucomannan/NFC composite films in the presence of CA. The impacts of the CA content and weight ratio of glucomannan and NFC on the mechanical properties, solubility, surface free energy and moisture vapor permeability (MVP) of the composite films were comparatively analyzed.

The moisture barrier property of hemicellulose-based films that are targeted for food packaging

is characterized by moisture vapor permeability (MVP). The function of the edible packaging or coatings that are made of biofilms is to prolong shelf life and maintain the product quality such as taste and texture. The uptake of moisture is an important factor on the rate of degradation of the product, therefore the films serving as moisture barriers are the crucial interest in the food industry.

There are two properties to assess the barrier properties of the films, which are the moisture vapor permeability (MVP) and oxygen transmission rate. The MVP is defined by gravimetrically measuring the transport of water through a film specimen. The water vapor transmission rate (MVTR) is defined as

$$MVTR = \frac{\Delta m}{\Delta t \cdot A} \quad (2.1)$$

where Δm is the change in weight, Δt is the elapsed time, and A is the area of the tested film.

The moisture vapor permeability (MVP) is defined as

$$MVP = \frac{MVTR \times L}{\Delta p} \quad (2.2)$$

where L is the film thickness and Δp is the difference in vapor pressure on the two sides of the

film.

2.6 Inks and Substrates for Printed Electronics

Printed electronics also requires advanced materials technology for substrates. The requirements include flexibility, excellent transparency in many cases, surface smoothness, features being thin and lightweight, with low thermal expansion, stiffness, heat resistance, low cost, among others. Several choices are available as substrates depending on the nature of the PE product. Substrates for PE may be flexible or rigid, porous, or nonporous. Table 1 lists materials commonly used in PE products.

Table 1 Materials Commonly Used as Substrates in PE [57].

Material	Thickness (μm)	Density (g/cm^2)	Transparency (%)	Haze (%)	Tg ($^{\circ}\text{C}$)	Process Temperature Limit ($^{\circ}\text{C}$)
PET	16-100	1.4	90	Approx. 0.3	80	120
PEN	12-250	1.4	87	Approx. 0.8	120	155
PI	12-125	1.4	-	-	410	300
Glass	50-700	2.5	90	0.1	500	400
Paper	100	0.6-1.0	-	-	-	130
NFC film	20-200	Approx. 1	90	1-2	200	150
Steel	200	7.9	-	-	-	600

A glass substrate is an attractive transparent substrate and has been widely used for most optical purposes such as displays, photovoltaic, and lightings. Its transparency is greater than 90 %, with a haze far below 1%. Thin glass substrates are now commercially available [58]. The thickness of glass substrates has already reached 30 μm . In contrast, the weakness of glass substrates is their brittleness, heavy weight compared with plastics, and high cost. To provide flexibility and robustness to PE products, plastic, paper, or steel substrates are in many cases better.

PET film is the most popular and widely used plastic film within the PE industry. It has high optical transparency above 90% and the great benefit of low cost compared with other substrates.

A known drawback pertaining to the use of PET is its poor heat resistance. Due to its poor heat capability, all printing process utilizing PET must be performed at low temperatures (below 130 $^{\circ}\text{C}$), and under low tension. The heat resistance gets better for polyethylene naphthalate (PEN) and much better for polyethylene (PE), however, with doing so their transparency decreases and costs increase. Though polymeric films are the first choice for PE products, several things must be carefully controlled to minimize distortion, especially for roll-to-roll printing. These factors, which must be controlled are the atmospheric conditions (temperature and humidity), tension,

and drying. Printers must also have some level of distortion detection and high-resolution imaging with high-speed web handling.

Transparent paper with nanofibrillated cellulose fibers is one of the most interesting substrates for PE technology, since it has a high transparency as PET films, low thermal expansion as glass, greater strength than plastic films and good elastic modulus close to that of steel [59]. The thickness of the nanopaper can be controlled from a few microns to several hundred microns using a conventional papermaking process. No polymer binder is required. Nanofibrillated cellulose, though quite expensive to make, is abundant and environmentally friendly because it is biodegradable and disposable. It was reported that the compatibility between silver nanowires and transparent paper is perfect [60].

Paper substrates are also attractive for PE technology. The major advantage of paper substrates is their low cost and disposability due to their biodegradability. Disposable devices, such as RFIDs on a paper substrate without a Si chip, are expected to establish one of the biggest PE application markets. Paper without any polymer addition will be the main biodegradable substrate. In addition, transparent nanofibrillated cellulose paper can provide display windows for paper

devices. Nanofibrillated cellulose paper possesses excellent optical properties. The transparency of nanofibrillated cellulose paper is almost equivalent to that of PET films and its heat resistance is similar to that of PET, as shown in Figure 5. The other attractive feature of transparent nanofibrillated cellulose paper is its low thermal expansion and high Young's modulus. The thermal expansion coefficient is close to that of glass, $8 \times 10^{-6}/^{\circ}\text{C}$, and the Young's modulus is approximately 140 GPa. These mechanical properties provide excellent dimensional stability [59].

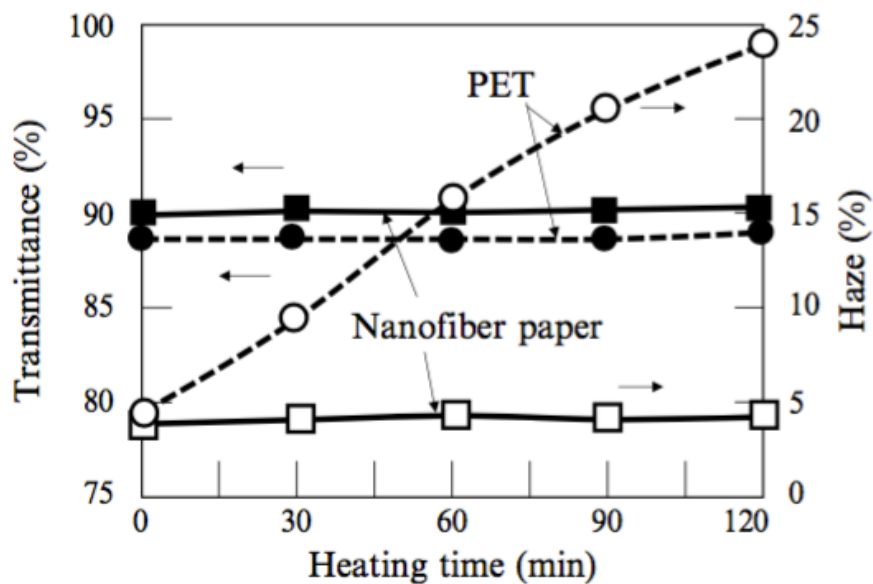


Figure 5 Transparency of Nanofiber Paper and PET Films [61]. Total Light Transmittance During Heating at 150 °C for 120 min (Solid Square: Nanofiber Paper; Solid Circles: PET) and Haze During Heating at 150 °C for 120 min (Square: Nanofiber Paper; Circles: PET).

2.7 Substrate Wetting and Ink Spreading

When it comes to printing, it is essential to understand the behavior of ink on the chosen substrate. Universally, surface energy is assigned to solids, while surface tension describes the liquid's shape change. Surface energy/tension is responsible for the surface composition of an isolated material (atmosphere-solid contact) and the wetting phenomena (liquid-solid contact). In the field of papermaking and printing, the last one is more attractive for the engineers. Wetting of a substrate can be easily observed by putting a drop of a liquid on the substrate, while observing its shape deformation with progressing time. If the shape of the drop flattens very quickly this would signify faster and greater spreading and wetting (water on the paper tissue). If the drop does not change its shape, or if it changes very slowly, this would signify non-wetting characteristics (droplets of rain on waxed car). To quantify the rate of wetting, the concept of contact angle must be understood.

Contact angle was first described by Thomas Young in 1805 [62]. Contact Angle (θ_C) is the angle measured between the liquid and the solid by drawing a tangent at the point of contact. Finally, contact angle is calculated by looking at the slope of the tangent to the drop at the liquid-solid-vapor (LSV) interface line [63].

There are multiple approaches how to calculate contact angle. If sessile drop shape is chosen, this calculation will involve Laplace Young equation. This equation applies when both solid surface and liquid drop are in equilibrium [64].

$$\gamma_{SV} = \gamma_{SL} + \gamma \cos \theta_C \quad (2.3)$$

Where:

θ_C : Contact angle

γ_{SV} : Solid-vapor interfacial energy

γ_{SL} : Solid-liquid interfacial energy

γ : the liquid-vapor energy (i.e. the surface tension)

Two unknown properties γ_{SV} and γ_{SL} are in the equation, but the approximate answers can be given by models based on independent knowledge of how liquids and solids adhere to one another. The biggest difference in models is how many different test liquids are required for a single estimation. A model widely used in industrial research is Owens-Wendt [65].

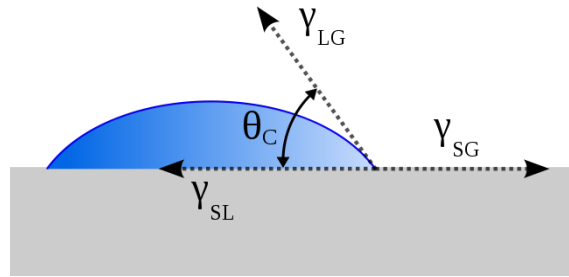


Figure 6. Contact Angle of Liquid on a Substrate [62].

Analysis of drop shape is a convenient way to measure contact angle and thereby determine surface energy/tension. This method assumes that the drop is symmetric about a central vertical axis, which means it is irrelevant to choose from which direction to view the drop. Moreover, another assumption is that the drop is not in motion, in the sense that viscosity or inertia are playing a role in determining its shape, indicates that the interfacial tension and gravity are the only forces shaping the drop [62]. Thus, the drop shape analysis can be applied.

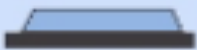




$\alpha = 0^\circ$		Spreading
$\alpha < 90^\circ$		Good wetting
$\alpha = 90^\circ$		Incomplete wetting
$\alpha > 90^\circ$		Incomplete wetting
$\alpha > 180^\circ$		No wetting

Figure 7 Contact Angle and Wetting Rate [61].

Besides the contact angle method, surface tension can be measured and expressed with the unit dynes/cm or mN/m. The testing methods contain pendant drop shape analysis, maximum bubble pressure, Wilhelmy plate method and du Nouy ring method. With FTA200, we can measure the surface tension by the analysis of pendant drop.

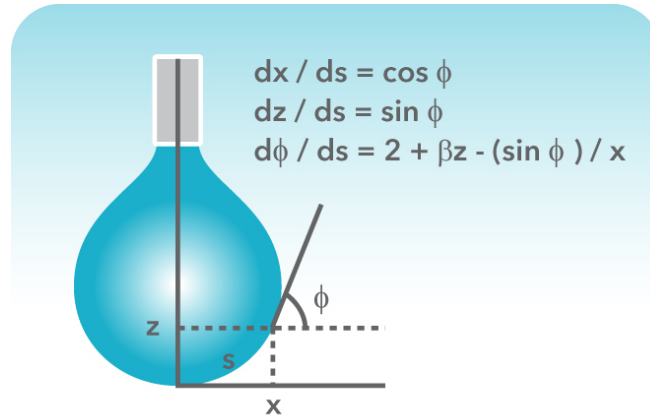


Figure 8 The Calculation of the Shape Factor β .

In this method, the pendant drop shape from a syringe tip is determined from the balance of forces, which include the surface tension of that liquid. The surface or interfacial tension at the liquid interface can be related to the drop shape through the following equation [65]:

$$\gamma = \Delta \rho g R_0^2 / \beta \quad (2.4)$$

Where: γ = surface tension

$\Delta \rho$ = difference in density between fluids at interface

g = gravitational constant

R_0 = radius of drop curvature at apex

β = shape factor (defined through the Young-Laplace equation expressed as 3

dimensionless first order equations as shown in Figure 8).

The iterative approximations in the software allow solution of the Young-Laplace equation for β to be performed. Thus, surface tension of the testing liquid can be measured with the known densities of two fluids. This method has advantages in that it is able to use very small volumes of liquid, measure very low interfacial tensions and can measure molten materials easily. High quality surface and interfacial measurements can be made with this method using an Attension Theta or Theta Lite optical tensiometer [64].

Low-surface-tension liquids will have a positive initial spreading coefficient but a near-zero, but negative final one; this comes about because the film pressure of the Gibbs monolayer is large enough to reduce the surface tension of the water-air interface to a value below the sum of the other two. Thus, the equilibrium situation in the case of organic liquids on water generally seems to be that of a monolayer with any excess liquid collected as a lens. The spreading coefficient $S_a(A)/A$ can be determined directly, and Zisman and co-workers reported a number of such values [65]. They called the value of the surface tension of the liquid that is equal to that of the analyzed material γ_c (critical surface tension). To obtain the value of γ_c , a series of contact angles is measured using liquids with progressively smaller surface tensions. The surface tension of

these liquids is then plotted against the cosine value of the corresponding contact angle.

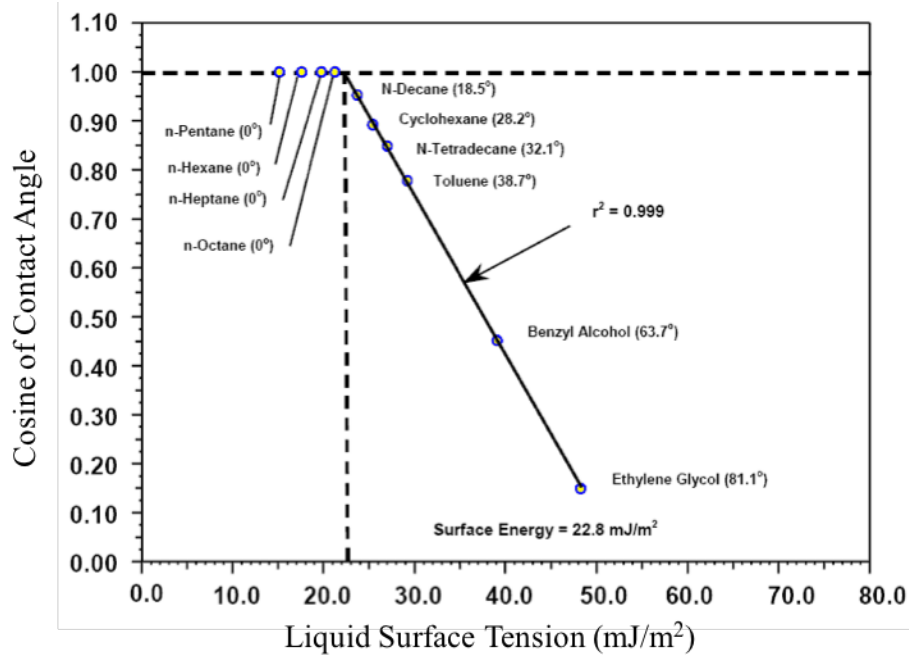


Figure 9 An Example of Zisman Plot [65].

The solid line in Figure 9 represents a best fit for the measured points and is extrapolated to intersect with the value of $\cos \theta = 1$. At the point of the intersection a line (dashed line) is drawn perpendicular to the x axis and a value of γ_c can be obtained. This protocol for obtaining γ_c is typically repeated for a variety of liquids; and qualitatively, at least, the critical surface tensions for homologous liquids, on the same surface is correlated.

2.8 Smart Packaging and Moisture Sensor

Sensor applications have gained importance due to the progress in information technology

infrastructure, which allows efficient handling of large data volumes. As the cost of sensor technology decreases with additive printing technology, the usage will spread to new market segments, including business areas with products that never before have carried such functionalities. For example, sensor technology is now used for cellulose-based products for packaging, hygiene, or graphical use [67]. The primary interest in the package application is to perform surveillance functions where the sensor technology enhances the primary function of the package, namely to protect the product it carries. Currently, there is also a growing interest to develop technology that allows objects to be interactive and integrated with digital services accessible on the Internet [68]. Such digital functionalities would further enhance the communication capability of the package and allow the package to become an access point or a point of sales display for a series of products related to the product itself or the brand of the product [69]. The digital communication channel can also be used to get feedback from or direct contact with the customer [70]. The information harvested can be used in further development of the product, or to build customer loyalty programs.

The package is a graphical medium and adding a digital functionality may further enhance the

story-telling capability of the product. The use of 2-D graphical codes, such as the QR code or Data-matrix code, or recent developed capacitive-code-compatible smart phone displays could provide a variety of new digital services [71].

The starting point for smart packaging solutions is surveillance and service functions in the supply chain. This includes sensor functions to monitor the transportation and storage of the product to guarantee that it has not been damaged [72]. A large application is packaging logistics where radio frequency identification (RFID) technology will play a major role. RFID tags can also carry sensor functionality to further increase transparency and traceability, where the major beneficiaries are the stakeholders along the entire supply chain [73]. A large part of the packaging business is extremely cost sensitive, and all together the package solutions and the supporting infrastructure will have to provide either a high added value or a very low cost. The total cost includes the system functionality, electronic label, and integration into the package. Thus, optimizing one aspect may increase cost in another.

Some moisture sensors are based on LC resonators [74] (L refers to the inductance and C represents the Capacitance in the equivalent circuit). The working principle of the printed

moisture sensor used in this study is based on planar interdigitated electrodes (IDE) [75] or finger structure [76] (Figure 10). A porous paper substrate has a large interfacial area, so it might provide higher sensitivity than the commonly-used polymers (e.g. polyimide) for a humidity sensor.

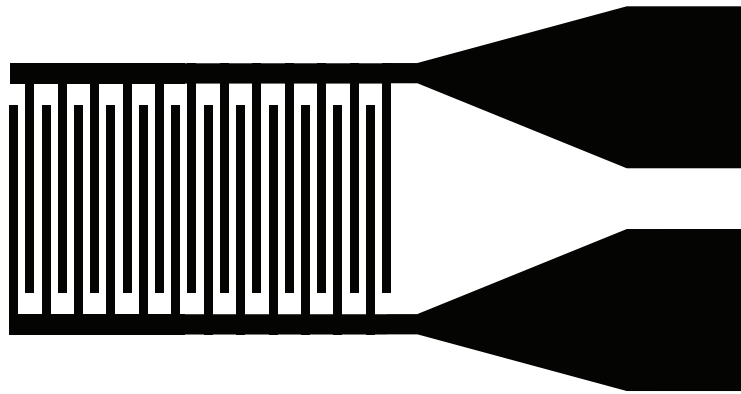


Figure 10 Schematic of the Layout of a Planar IDT moisture sensor [75].

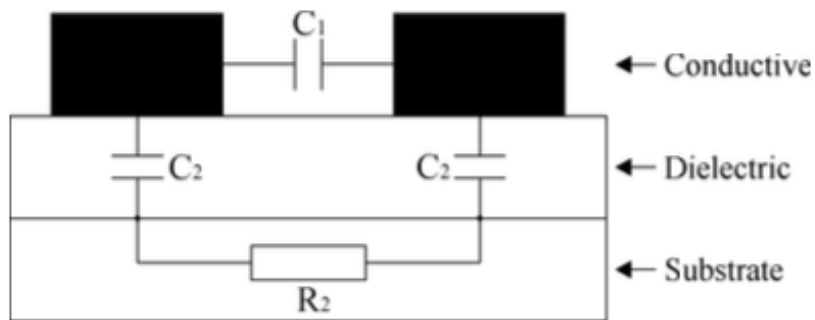


Figure 11 A Cross Section of the Moisture Sensor, with the Moisture Sensitive Substrate, the Dielectric Layer and the Conductive Sensor Layer [76].

The sensor solution for measurement of moisture content in cellulose-based substrates is built up through three layers as shown in Figure 11. First, there is a substrate that changes its conductivity when it is exposed to moisture. Second, because of this conductivity change in the substrate, a dielectric or insulating layer is required to ensure that there is no short circuit in the conductive third layer. Third, there is a finger structure made out of a conductive film or printed conductive ink. The concept of the sensor solution is to measure the impedance in the interdigitated electrodes circuit.

The works described above provide the groundwork for further research into the use of hemicellulose-based biopolymers and barrier coatings for use in smart packaging applications.

As discussed above, hemicellulose combined with nanofibrillated cellulose is especially important for the development of biocompatible devices. Therefore, continual research is of interest to material suppliers, device designers and printers alike. As a consequence of the knowledge needed to use hemicellulose and nanofibrillated cellulose widely for packaging applications, this research aims to provide knowledge of the mechanical properties, surface properties, barrier properties and printability characterizations pertaining to the development of

PE devices for smart packaging. To accomplish this goal, three studies were conducted, and are discussed below.

CHAPTER 3

PREPARATION AND CHARACTERIZATION OF HEMICELLULOSE-BASED FILMS

3.1 Abstract

Flexible plastic films such as PET, LDPE and PET have been the most common substrates used in the printing and packaging industry for the last few decades. However, the global sustainability calls for more environmentally friendly, biodegradable and biocompatible materials. This research aims to advance the knowledge of the material properties of hemicellulose-based biofilms. Laboratory preparation of the hemicellulose-based films and the characterization of mechanical and surface properties were done. The biodegradable glucomannan films were formed with or without nanofibrillated cellulose (NFC). In all cases, nanofibrillated cellulose improved mechanical properties of the films. Gravure printing was demonstrated on the biofilms. The one-way ANOVA method was used to analyze the effect of glucomannan, sorbitol as a plasticizer, and nanofibrillated cellulose on the mechanical properties of the films. It was found that all of those factors significantly affected the mechanical properties of the biofilms.

3.2 Introduction

Flexible PET (Polyethylene Terephthalate) or LDPE (Low-density polyethylene) films are currently the main substrates for food and pharmaceutical packaging. Plastics have been the dominant packaging materials because of their much better barrier properties compared to traditional paper packaging. However, the common plastic films can't be easily degraded, which causes serious pollution and sustainability issues. For example, the incineration of some plastics such as PVC increases dioxin and furan content of air emissions. Therefore, the global sustainability focus relies more on biodegradable and biocompatible materials. Natural polymers, such as polysaccharides, are ideal starting materials for these kinds of composites due to their biodegradability, biocompatibility, non-toxicity and renewability [77]. However, films made of pure hemicelluloses lack flexibility and have poor thermo-mechanical properties, thus they need to be modified. Xylan films alone without modification are brittle, but they can be derivatized to reach decreased water uptake, and increased flexibility. Enhanced mechanical properties of hardwood xylan films can be improved with addition of nanofibrillated cellulose, nanocrystalline cellulose [78,79], and sorbitol as a plasticizer [80], or a plant protein such as gluten [81]. Micro-

and nanofibrillated celluloses were successfully applied for film reinforcement in composite materials [82]. Hemicelluloses may be obtained from plant material by chemical or by gentler enzymatic treatments [83], or a combination of both. Obviously, the original source of xylan, or other hemicelluloses can dramatically affect mechanical properties of composite films [84]. Linear xylans are available from corncobs, glucuronoxylans from hardwoods, arabinoxylans from barley, oat, rye, and other cereal brans [85-87]. Depending on the particular plant material, the chemical composition of hemicelluloses vastly differs, as shown in Table 2 [86].

Table 2 Hemicelluloses and Their Sources [86].

Type of hemicellulose	Source	Amount (%)
Arabinoglucuronoxylan	Softwood	7-10
Arabinogalactan	Larchwood	5-35
Arabinoxylans	Annual plants, bran	Variable
Galactoglucomannan	Softwoods	20
Glucomannan	Hardwood	2-5
Glucuronoxylan	Hardwoods	15-30

Biodegradable films have been prepared from galactoglucomannans and xylans isolated from wheat straw and blended with carrageenan and locust bean gum [88]. Film-forming properties of xylan hemicelluloses can be enhanced by acetylation [89], or by reinforcing with cellulose nanofibrils. Galactoglucomannans have been hydrophobized and used for packaging

applications, too [90].

Lignocellulosic biomass from trees, annual grasses, cereals, and other plants have become the main focus of the developing a bio-refining industry [91]. As the main components of plants, cellulose, lignin and hemicelluloses have received a lot of attention in terms of material applications. Hemicellulose is defined as the alkali-soluble polysaccharide remaining after the elimination of pectic substances from plant cell walls [92]. Hemicelluloses (Figure 12), depending on their plant material source and sugar composition, can be divided into five main groups, which can be defined according to their primary structure as follows: arabinoglucuronoxylans, galactoglucomannans, arabinogalactans, glucomannans and glucuronoxylans [93,94].

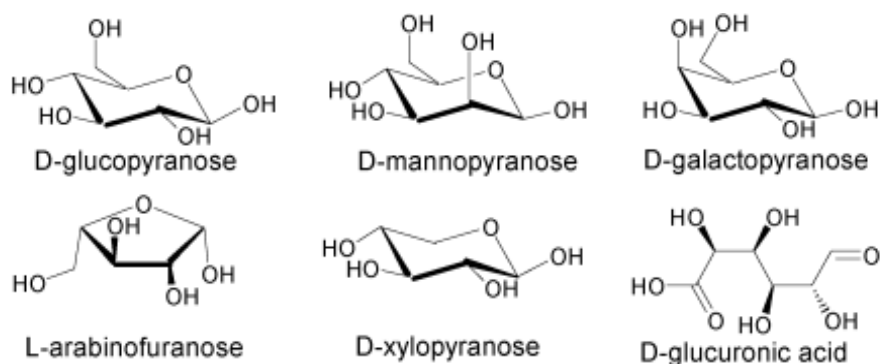


Figure 12 The Main Components of Hemicelluloses [92].

The research on hemicelluloses and their packaging and medical applications has been extensive.

The konjac glucomannan, which is derived from the plant of genus *Amorphophallus* has been used commercially for many years because of its gel- and film-forming properties and the biocompatibility and biodegradability [93]. There are several ways to obtain hemicelluloses from plant resources, including extraction with alkali, dimethyl sulfoxide or methanol/water, as well as steam or microwave treatment [95]. Depending on different pretreatment procedures, the composition of the hemicelluloses could be varying. Sun et al reported the dependency of composition on the isolation procedure, as the pretreatment of wheat straw samples with various organic solvents before extraction resulted in very different hemicellulose products [96].

Hemicelluloses are hydrophilic in nature, hence hemicellulose-based films are generally hygroscopic, which means they will absorb moisture and degrade with high humidity. This is because they have abundant free hydroxyl groups distributed along the main and side chains and they are ideal candidates for chemical functionalization. Many researchers have been focusing on modifying the properties such as crystallinity, solubility and hydrophilicity of hemicelluloses through techniques such as esterification, etherification or grafting methods. Through the chemical modifications, the hemicellulose-based films could have lower oxygen permeability,

lower water vapor permeability and higher mechanical strength and flexibility. Grondahl et al. reported the films made of glucuronoxylan from aspen wood show improved oxygen barrier properties and the addition of plasticizer resulted in increasing tensile strength [97].

Hemicelluloses, besides cellulose and lignin are main components of the plant cell wall and are bound to lignin. The compositions of hemicelluloses are different depending on various raw materials. For example, a study from Lai et.al. reported that the main components vary a lot in four kinds of rice straw, containing arabinose (5%-23%), xylose (17%-40%), and glucose (36%-55%) [98].

The films that are made on the basis of hemicellulose with addition of plasticizers were reported as early as 1949 by Smart and Whistler [99]. The reason to use plasticizers in hemicellulose-based films is to ensure flexibility and the most commonly used plasticizers are sorbitol, glycerol and xylitol (Figure 13). Besides packaging applications [100] biodegradable hemicellulose films can be used for biomedical applications because of their non-toxicity, biodegradability, and biocompatibility [101]. Biomedical applications include controlled drug release or improved medical imaging [102].

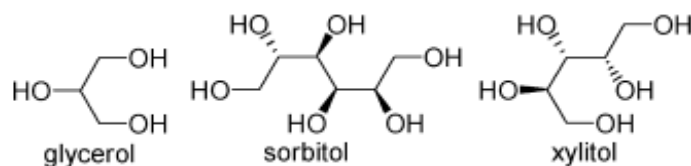


Figure 13 Commonly Used Plasticizers for the Hemicellulose-based Films [93].

In this work, the biodegradable glucomannan films were formulated with and without nanofibrillated cellulose, with the aim to reinforce the mechanical strength of the film and impart the film with improved barrier properties. Another aim was to characterize selected physical properties of formulated films and assess possible printability.

3.3 Experimental

Glucomannan from NOW Foods, Inc. (Figure 14) solution (0.5%-1% w/w) was prepared in a 250 ml beaker during continuous stirring at 25 °C. Nanofibrillated cellulose (NFC contains: Water 95%-99%, Cellulose pulp 1-5%; manufactured by the Department of Chemical and Biological Engineering, University of Maine) in suspension form was added to the glucomannan separately. Then 1% lignin in powder form with 95% purity (Sigma Aldrich) and 0.1% Surfynol® CT111 (Air Products and Chemical, Inc.) were added.

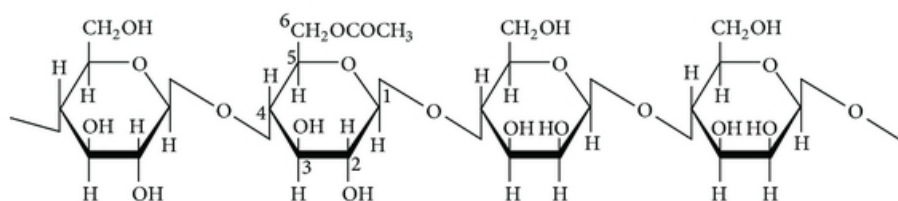


Figure 14 Glucomannan Composed of β -D-Glucopyranose and β -D-Mannopyranose Units Linked by 1 \rightarrow 4 β -D- Glycosidic Bonds (Second Glucopyranose Unit is Esterified) [98].

The formulations of the films (Table 3) were designed with different dosage of NFC, glucomannan and plasticizers, with the purpose to decide how they affect strength properties.

The mixture was further homogenized using a magnetic stirrer (Corning Model PC-420) at 45 °C at a mixing speed of 600 RPM. The solutions were casted to a mold with the dimensions of 100 mm \times 100 mm. Films were dried in the Environmental Test Chamber (Caron Model 6010; temperature range: 5 °C to 70 °C; humidity range: 20% to 98% RH) for 8 hours at 60 °C and 35% RH). Dried hemicellulose-based films were peeled off manually and stored in polyethylene bags prior to characterization.

Table 3 Formulation of Biofilms.

Ingredient (g)	Film 1	Film 2	Film 3	Film 4
Water	100	100	100	100
Xylan	1	1	0	0
Sorbitol	0.5	0.5	0	1
Glucomannan	0.5	1	0.5	1

Lignin	1	0	0.5	1
NFC	0	0.1	0	0.2
Surfactant	0.1	0.1	0.1	0.1

Selected mechanical properties, and surface energy of the films were tested. The PET film (from Dupont LLC.), along with uncoated paper with a basis weight of 118 g/m² (from Western Michigan University Pilot Plant) were also analyzed as a control sample. For each test five replicates were done per each film.

When it comes to printing, it is essential to understand the behavior of ink on the chosen substrate. Surface energy/tension is responsible for the surface behavior (atmosphere-solid contact) and the wetting phenomena (liquid-solid contact) (Figure 6) [63, 65].

The surface energy of the films was estimated by the FTA200 (First Ten Angstrom Dynamic Contact Angle) measurement apparatus. Pendant drop analysis was used for the surface tension measurements of liquid phases. Sessile drop analysis was used for the contact angle measurements. The actions of the droplet appear live on the computer screen and the salient images are captured to the computer's memory for later image analysis. The camera frame rate is 60.9 frames per second. The surface energy is calculated by the program by using Owens-Wendt method using 1 angle of each of 2 liquids on 1 solid. For each kind of liquid, the software

captured 300 images of the fluid dropping, hitting the substrate and reaching and equilibrium on the substrate.

The FTA200 is a flexible video system for measuring contact angle, surface and interfacial tensions, wettability, and absorption. For the evaluation of the surface energy, the contact angle of three liquids, deionized ultra-filtered water (DI), hexadecane, and methylene iodide (MI), were measured against the biofilm surfaces, and the critical surface free energy was calculated using Owens-Wendt method [65]. Although these methods only estimate the solid surface energy, such values are useful for comparing the wettability of solid surfaces and predicting print adhesion.

Contact angle measurement is the ideal method for the characterization of surface energy and surface wettability and is a widely used technique for studying the loss and recovery of hydrophobicity of the films. Therefore, this method can be used to accurately measure the hydrophilic characteristic of a surface of a hemicellulose-based film. This method enables the surface energetics of a solid surface to be determined by its free surface energy. Often, it is defined on the basis of the static contact angle between the surface and a liquid droplet. The

fundamental equation for measurement of solid surface tension by contact angle measurements is described by the Young's equation (Equation 2.3) [63]. Contact angles of deionized ultra-filtered water (DI), hexadecane, and methylene iodide (MI), were measured against the biofilm surfaces, and the critical surface energy was calculated using Owens-Wendt method measurements on a solid substrate (Table 3.5) [65].

The tensile strength and elongation at break for the films were assessed according to TAPPI Standard T494 at 23 °C and 50% RH using an INSTRON 430I with a 500 N load cell. The specimens were conditioned under 23 °C and 50% RH for 24 hours prior to testing. The initial gauge length was 100 mm, and the crosshead speed was 25 mm/min. The width of each specimen was 15 mm.

The bursting strength of the biofilms was measured using the Mullen Tester according to TAPPI Standard T403.

Gravure printing was demonstrated with a laboratory gravure proofing press K-Printing Proofer (Testing Machines Inc.) at a speed of 40 m/min. The image on the plate is a solid patch with a fine resolution of 200 lines per inch. The black gravure ink was acquired from Western Michigan

University pilot plant. The ink is toluene based with a viscosity of 15 centipoise. The printed films were placed in the laboratory at controlled conditions (23 °C, 50% RH) for 24 hours conditioning prior to optical density measurement with an X-Rite eXact SpectroDensimeter. The density measurement conditions are in absolute mode with statue T, with a white backing.

3.4 Results and Discussion

Four different hemicellulose formulations (Table 3) were designed with different dosage of NFC, glucomannan and plasticizer, with the aim to decide how they affect strength properties of resulting films and evaluate their printability. Films were formulated with various amounts of xylan, glucomannan, nanofibrillated cellulose, lignin, sorbitol, and surfactant. It was observed that the xylan and lignin make the films more brittle, and on the other hand, nanofibrillated cellulose showed strengthening effect of the films. To find out how if individual components are statistically important and how they affected strength of the films, ANOVA analysis was performed.

3.4.1 Optimization of Biofilm Formulation

The main factors in the film formulations are the portion of nanofibrillated cellulose, sorbitol and glucomannan. In order to analyze the results of the film formulation, a one-way ANOVA of Tensile versus the main factors, was performed using the Minitab® 17 software package (Minitab Inc.). The full ANOVA was not performed because of not enough degrees of freedom for given factors. ANOVAs were performed on the data pertaining to nanofibrillated cellulose content versus tensile strength, sorbitol as a plasticizer amount, and level of glucomannan added (Table 4). The significance level for each ANOVA is set as 0.05. The results are shown in the Table 5.

Table 4 The Factors and Levels in ANOVA Analysis for the Film Formulations.

Factor	Level (mass fraction %)		
NFC	0	0.1	0.2
Sorbitol	0	0.5	1
Glucomannan	0.5	1	N/A

Table 5 ANOVA for Tensile Strength Versus Nano-fibrillated Cellulose (NFC).

Source	Degree of Freedom	Adj. SS	Adj. MS	F-value	P-value
NFC	2	0.00644	0.00322	176.88	0.000
Error	12	0.00022	0.00002		
Total	14	0.00666			

Although the preliminary formulations of the biofilm represent an unbalanced design, it is instructive to investigate which factor contributes to the tensile strength and thus optimize the film formulation design in the future work. For nanofibrillated cellulose and sorbitol, there are 3 levels of the factor and 5 replicates for each level. For glucomannan, there are 2 levels and 5 replicates for each level (Table 4). The program computed the F ratio F-Value equals to 176.88 and we can compare this result to an appropriate upper-tail percentage point of the $F_{2,12}$ distribution. Suppose the $\alpha=0.05$, $F_{0.05,2,12}=3.89$ [104]. Because $F_0=176.88>3.89$, we reject H_0 and conclude that the treatment means differ, that is, the amount of nanofibrillated cellulose significantly affects the mean tensile strength of the films. For the tensile strength versus sorbitol, the $F_0=216.62>F_{0.05,2,12}=3.89$, which means the amount of sorbitol also significantly affects the mean tensile strength of the films (Table 6). For tensile strength versus glucomannan, the $F_0=165.5>F_{0.05,1,8}=5.32$, which means the amount of glucomannan significantly affects the mean tensile strength of the films, too (Table 7) [104].

Table 6 The ANOVA Table for Tensile Strength versus Sorbitol.

Source	Degree of Freedom	Adj. SS	Adj. MS	F-value	P-value
--------	-------------------	---------	---------	---------	---------

Sorbitol	2	0.01264	0.00632	216.62	0.000
Error	12	0.00035	0.00003		
Total	14	0.01299			

Table 7 The ANOVA Table for Tensile Strength versus Glucomannan.

Source	Degree of Freedom	Adj. SS	Adj. MS	F-value	P-value
Glucomannan	2	0.00388	0.00388	165.50	0.000
Error	12	0.00019	0.00002		
Total	14	0.00407			

3.4.2 Strength Properties

Tensile tests measure the force required to break the sample specimen and the extent to which the specimen stretches or elongates to that breaking point. The tensile strength data can help specify optimal film formulations. Tensile strength of the films is shown in Figure

15.

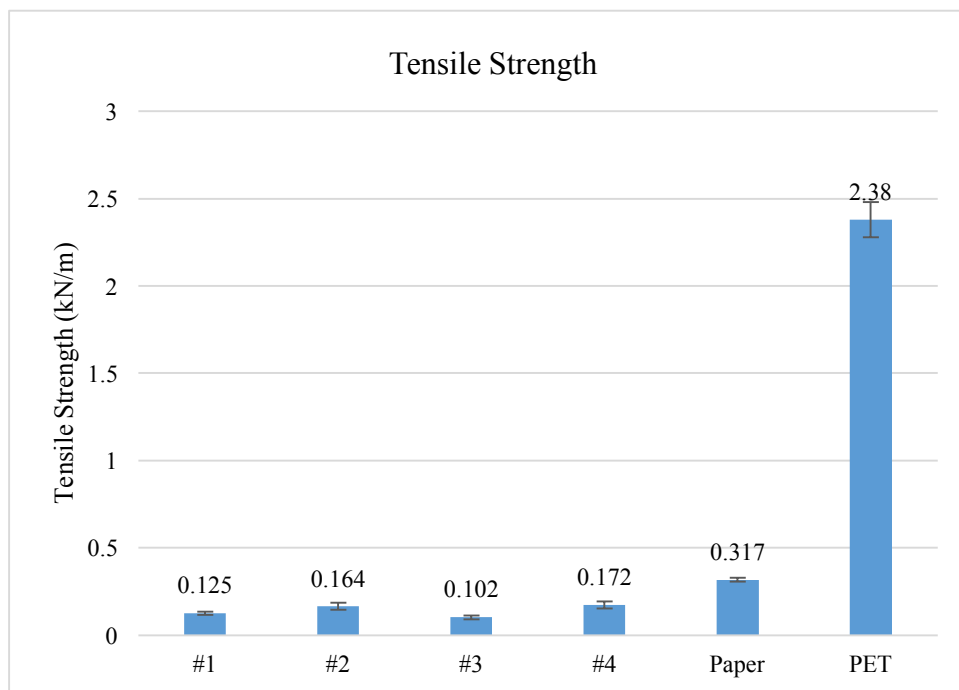


Figure 15 The Tensile Strength of the Hemicellulose Based Films, Paper and PET Film.

Compared to xylan and lignin, nanofibrillated cellulose has a clearly better strengthening effect on the films. The tensile strength of the hemicellulose films is much lower than PET film, but it is relatively comparable with the kraft paper. Among the four hemicellulose film formulations, the film #4 had the highest tensile strength, probably due to highest addition of nanofibrillated cellulose. Film #1 made with lignin and sorbitol lacks flexibility. Film #3 made with glucomannan and lignin without plasticizer was brittle.

Elongation is the ratio between changed length and initial length after breakage of the test material. It expresses the capability of a material to resist the changes of shape without crack

formation. For elastomers and packaging films (e.g. LDPE), the ultimate elongation values could be several hundred percent. For rigid plastic, such as fiber reinforced PET films, the elongation values are under 5%. The combination of high tensile strength and high elongation leads to materials of high toughness. Elongation of hemicellulose biofilms was larger than that of paper (Figure 16), but much less than PET film. The highest elongation was found at film formulation #4 with the highest amount of nanofibrillated cellulose.

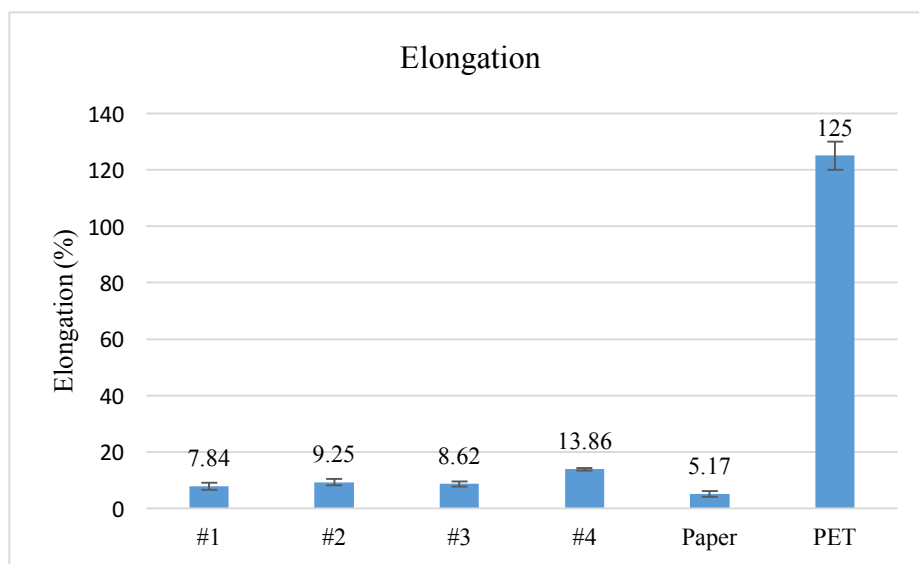


Figure 16 The Elongation of the Hemicellulose-based Films, Paper and PET Film.

The bursting strength is defined as the hydrostatic pressure needed to burst a sample when it is applied uniformly across its side. The bursting strength is measured by using a rubber diaphragm

that is expanded hydraulically against the sample. Bursting strength tests are generally used for paper and board where there are definite warp and weft directions due to the fiber bonding. However, the biofilms were casted onto an aluminum foil covered mold. It was like a handmade sheet in the laboratory without obvious orientation. In other words, the film is homogeneous, which means during bursting test, the film undergoes the same extension in all directions. This could be proven by the uniform rupture of the film samples. The bursting strength of the biofilms were close to the kraft paper, which could be an evidence for the statement that those films could function as packaging materials. Among all the formulations, film #4 has the highest bursting strength, which is coherent with its highest tensile strength. However, there is still long way to go for all the biofilms to be comparable with the PET film (Figure 17).

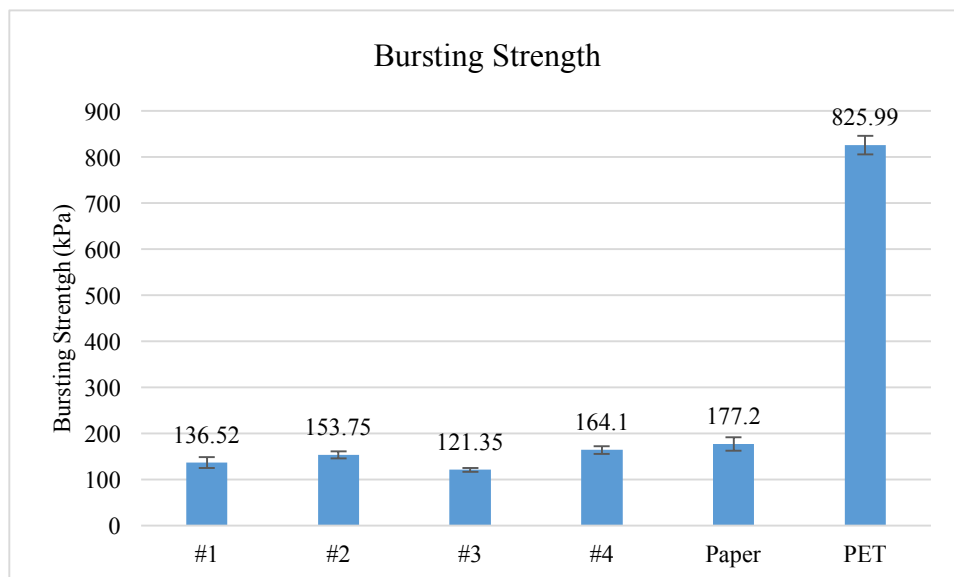


Figure 17 The Bursting Strength of the Hemicellulose-based Films, Paper, and PET Film.

3.4.3 Air Permeability

Permeability describes how easily a fluid is able to move through the porous material. It is calculated using a formula widely known as Darcy's Law [103].

Darcy's Law

$$Q = K \Delta P A / \eta \Delta L \quad (3.1)$$

Where

Q = flow rate (m^3/s); K = permeability coefficient, (m^2)

ΔP = pressure drop or difference, (Pa); L = flow length or thickness of test sample, (m)

A = area of cross-sectional area to flow, (m^2); η = fluid viscosity, (Pa-s)

The standard parameters for the PPS tester used were as follows [105]:

Fluid (air) viscosity (η): 1.80075×10^{-5} Pa-s (Ns/m^2) at 23°C

Standard pressure drop (ΔP): 6.17 KPa; Area of cross-section (A): 0.001 m^2

Therefore, the permeability coefficient [106] is,

$$K (\mu\text{m}^2) = 0.048838 * Q (\text{ml}/\text{min}) * L (\text{m}) \quad (3.2)$$

An example calculation of the permeability coefficient for a hemicellulose-based film using equation (3.2) follows:

Parker Print Surf flow rate (Q) at 1000 KPa: 0.59 ml/min

Thickness of the sample film (L): 223.6 μm

Permeability coefficient $K = 6.44 \text{ nm}^2$

Air permeability is a good measure of how much and how quickly inks are absorbed into a substrate. However, plastic films are considered non-porous substrates due to their low porosity (and permeability) in terms of both air and liquid penetration. This non-porous property enables the films to function as packaging substrate for special products such as foods, pharmaceutical products and chemicals. All the films are non-porous (Figure 18), which means that films have potential to serve as food packaging with good barrier property.

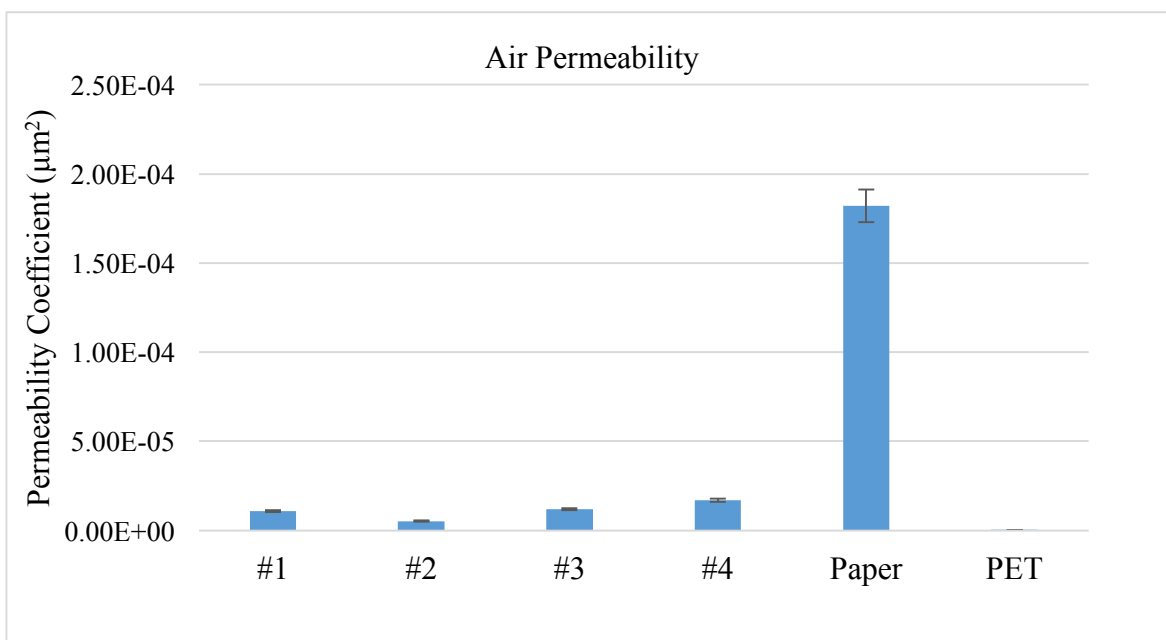


Figure 18 The Air Permeability of Hemicellulose-Based Films, Kraft Paper and PET Film.

3.4.4 PPS Roughness

For the contacting-type printing processes, such as offset lithography or gravure printing, the ink film will transfer to the substrate surface upon physical contact. When the voids in the substrate surface are deep enough to prevent such contact, or the substrate is too rough, ink transfer will not be uniform and will cause poor print quality. The roughness (R_a) of the biofilm was measured using the Messmer Parker Print-Surf (PPS) with soft backing and 1000 kPa clamping pressure. Compared to film #1, the surface of the films #3 and #4 are less even (Figure 19).

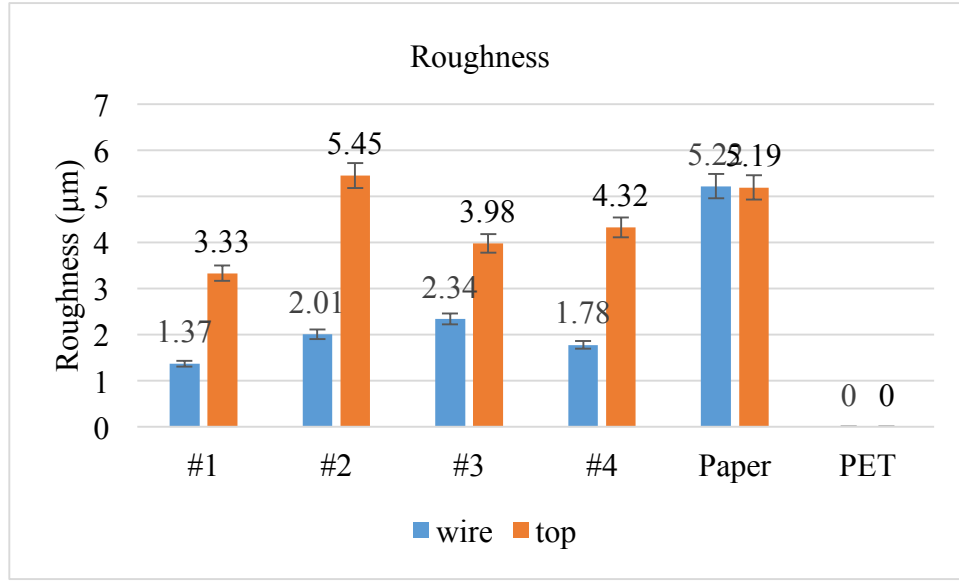


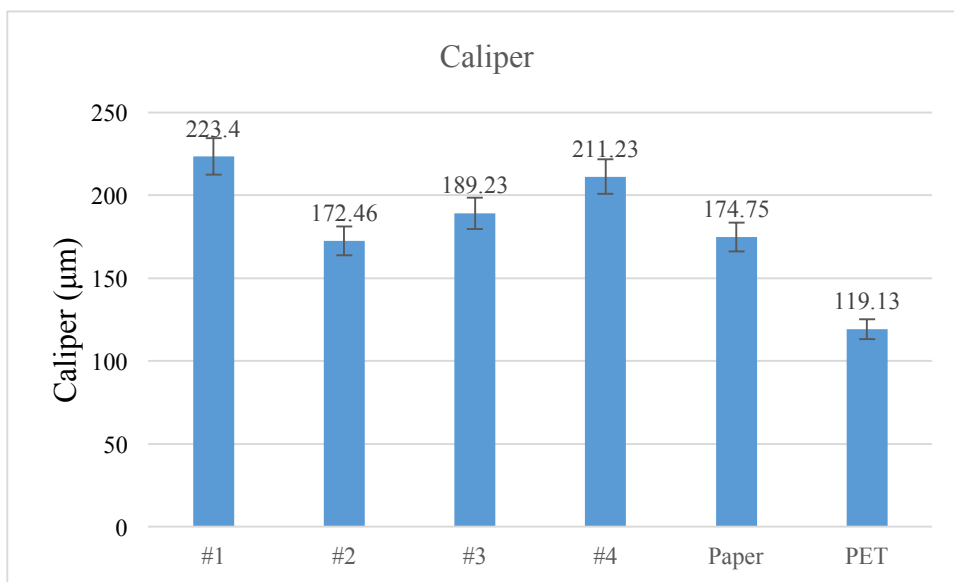
Figure 19 The Roughness of Hemicellulose-based Films, Kraft Paper and PET Film.

This is due to the bubbles that were introduced to the suspension during mixing and drying of film forming process. The wire side is smoother than the top side due to its contact with the supporting foil backing. The top side has many tiny bubbles that were introduced to the suspension during mixing and spreading process, which leads to a rougher surface on the top side and make it more difficult to print on.

3.4.5 Caliper

The caliper of the biofilm was measured by Technidyne PROFILE/Plus Thickness instrument.

The caliper of the film was controlled during the film formation by using the Meyer rod, in this



case Meyer rod #46.

Figure 20 The Caliper of Hemicellulose-based Films, Kraft Paper and PET Film.

Films with NFC (#2 and #4) had higher amounts of glucomannan than films #1 and #3 (Figure 20), but lower caliper than the films without NFC (#1 and #2). It appears that NFC is responsible for better conformation and bonding of biofilm. The thickness of the films slightly increased with the amount of added NFC (film #2 and #4).

3.4.6 Surface Free Energy

Table 8 shows the surface tension of the liquid phases. Table 9 shows the contact angles on the biofilm substrate measured with the liquid phases. The surface tension values in Table 8 and the contact angle values in Table 9 were entered to the FTA32 software, in which the Owens-Wendt method requires contact angle of each of two known liquids on the substrate to estimate the surface energy. The surface energy results of each liquid pair- MI/DI and DI/HE, were calculated by the software and presented in Table 10. The Owens-Wendt equation resulted in slightly different surface energy values for the same substrate when the probe liquids were paired differently.

Table 8 Surface Tension of Liquid Phases with Values of Dispersion and Polar Components Used in Owens-Wendt Calculations.

Liquids	γ_{LV}	$\gamma_{LV-Disp.}$	γ_{LV_Polar}	Density (g/cc)
DI water (DI)	71.36±0.87	21.80	49.60	1.000
Diiodomethane (MI)	48.03±0.60	45.73	2.30	3.325
Hexadecane (HE)	21.30±0.26	21.30	0	0.770

Table 9 Owens-Wendt Method of Estimating Surface Free Energy Values of Hemicellulose Film #4 (DI- distilled water, MI- methylene iodide).

Owens-Wendt	Total (mJ/m ²)	Dispersive (mJ/m ²)	Polar (mJ/m ²)
-------------	----------------------------	---------------------------------	----------------------------

DI / MI	55.33	32.49	22.83
MI / Hexadecane	51.49	21.10	30.39

Because the mechanical test (tensile, bursting) showed that #4 film formulation produced the strongest film, therefore the #4 film was selected to perform the surface energy test, along with the PET and paper as control groups (Table 10 and Table 11). Estimated surface free energy value of 55.33 mJ/m² is relatively high, which predicts excellent wetting with ink and high ink adhesion. Hemicellulose is hydrophilic in nature, hence hemicellulose-based films are generally hygroscopic, which means they will absorb moisture. The water drops spread on the films and totally wet the surface. However, the methylene iodide drops bead up on the film surface. This is because the hemicellulose has abundant free hydroxyl groups distributed along the main and side chains and is affinitive to water.

Table 10 Owens-Wendt Method of Estimating Surface Free Energy Values of PET Film (DI- distilled water, MI- methylene iodide).

Owens-Wendt	Total (mJ/m ²)	Dispersive (mJ/m ²)	Polar (mJ/m ²)
DI / MI	45.80	38.70	7.10

Table 11 Owens-Wendt Method of Estimating Surface Energy Values of Kraft Paper (DI- distilled water, MI- methylene iodide).

Owens-Wendt	Total (mJ/m ²)	Dispersive (mJ/m ²)	Polar (mJ/m ²)
DI / MI	60.88	1.76	59.12

3.4.7 Printability Analysis

Preliminary printing experiments were done using K-Printing Proofer in gravure mode, mimicking rotogravure printing. Optical densities of the printed films are illustrated in Figure 21.

With similar surface free energy to the paper, the biofilm has higher print density with the same solvent based (Toluene) black gravure ink. This is probably due to the lower roughness of the film surface and lower air permeability of the film compared to the paper. Further study will investigate the topography of the biofilm surface by using the Bruker white light interferometer.

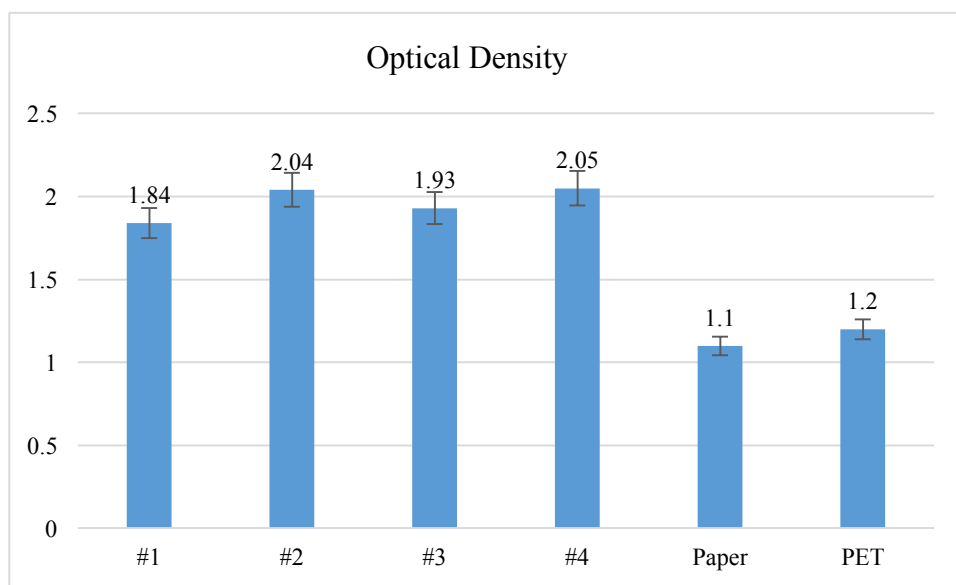


Figure 21 Optical Density of Solid Patch Printed on Glucomannan Films, Paper and PET Film.

3.5 Conclusions

Biodegradable glucomannan films were formulated with and without reinforcement with nanofibrillated cellulose. Statistical analysis of individual components addition showed that glucomannan, sorbitol and nanofibrillated cellulose all significantly affected mechanical properties of films measured as tensile strength. Nanofibrillated cellulose increased the mechanical strength of glucomannan films, which was attested by the increased tensile and bursting strength. The glucomannan films were relatively non-porous, which may be useful property with a potential use as a food packaging material with good integrity. The surface energy of the hemicellulose films was found to be relatively high because the hemicellulose is hydrophilic in nature. High surface energy of films was beneficial for ink adhesion. The films were gravure printed with solvent based ink using gravure K-proofing press. Print density of hemicellulose films were higher than those found on kraft paper and PET film. Thus, biofilms exhibited potential to be used as printed packaging materials.

CHAPTER 4

BIOPOLYMER FILMS FROM GLUCOMANNAN: THE EFFECTS OF CITRIC ACID CROSSLINKING ON BARRIER PROPERTIES

4.1 Abstract

Glucomannan extracted from konjac root is used to form biodegradable films with gas and grease barrier properties for food packaging application. Nanofibrillated cellulose (NFC) and plasticizers were used to improve the strength properties of the films. Citric acid and sodium hypophosphite (SHP) were used as crosslinking agents and catalysts to improve the barrier property of the films against moisture. The film samples were prepared from glucomannan and NFC using a dispersion-casting method. The moisture barrier properties were characterized by the moisture vapor transmission rates (MVTR) and showed a significant moisture vapor transmission rate decrease of 49.7% (CA35-C) upon citric acid and SHP addition. The crosslinked glucomannan films were calibrated with increasing mean tensile strength, modulus and elongation.

4.2 Introduction

Biopolymers are potential alternative sources for production of fuels and packaging materials

because they have the capability to be degraded or broken down through the action of naturally occurring organisms leaving behind organic by-products [107]. The most common and suitable biopolymers for food packaging applications are naturally occurring materials, such as cellulose, hemicellulose, starch, chitosan and agar. It was recorded that the global bio-plastic demand was 1.4 million metric tons in 2014; and it is expected to reach about 6 million metric tons in 2019 [108]. According to studies by Helmut Kaiser Consultancy [109], bio-plastics are expected to cover approximately 25-30% of the total plastic market by 2020.

The hydrophilic nature of polysaccharide films offers them good oxygen barrier properties, but their water vapor barrier and moisture resistance are relatively poor in comparison with the petroleum-based plastic films [110], which limits their potential application in packaging materials [111]. A high water solubility obviously affects the functionality of hemicellulose-based films as packaging materials. The hydrophilicity of the polysaccharides results in water swelling and impairs their mechanical and barrier properties [112].

Many studies on hemicellulose-based films report that the water resistance of the films can be improved by chemical or physical crosslinking, during which the polymer chains are crosslinked

by covalent bonds (chemical bonds) or weaker physical bonds. The crosslinking reagents could be dicarboxylic or polycarboxylic acids such as citric acid. The crosslinked hemicellulose form three dimensional networks that reduce the mobility of the structure, usually enhancing their water resistance (Figure 22), reducing both water solubility and swelling by water, and boosting their mechanical and barrier properties [113].

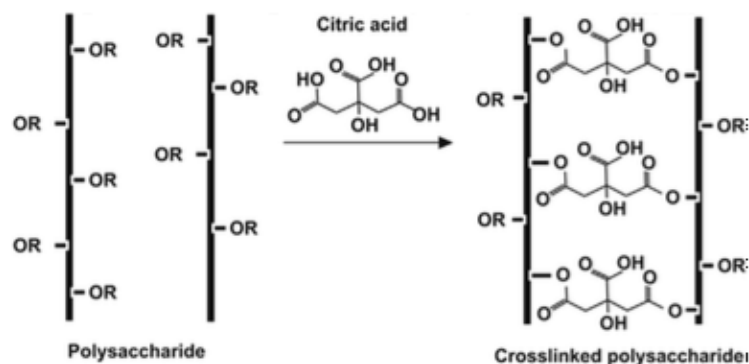


Figure 22 Mechanism for Covalent Crosslinking [113].

Hemicellulose and nanofibrillated cellulose are highly promising biopolymers for the production of packaging materials, since they offer films with good tensile and gas barrier properties [114]. In addition, they are renewable, available at low cost, and fully biodegradable. However, non-plasticized hemicellulose films are brittle and their hydrophilic character results in poor moisture barrier properties and high water sensitivity compared with petroleum-based plastic films such as

polyethylene or polypropylene. A common way to improve the film formation and hydrophobic properties is chemical modification, such as crosslinking. Plasticizers such as water, xylitol or sorbitol reduce the glass transition temperature, T_g , of the polymer matrix and prevent the formation of cracks and pinholes [115-117].

Glucomannan has shown good film forming capacity, which offers good barrier properties towards air and grease. Several research works and patents have indicated that the development of glucomannan-based films and coatings as sustainable printable packaging materials is commercially promising [118]. In the year of 2013, another new patent assigned by Xylophane came out dealing with a method for the production of flexible films or coatings for packaging based on hemicelluloses combined with a crosslinking agent or hydrophobizing agent, to be used as an oxygen, aroma, and /or grease barrier with improved moisture resistance [119].

Nanofibrillated cellulose, or NFC, is a biodegradable film-forming material widely studied for its industrially interesting properties and possible applications in food packaging. Various applications of nanofibrillated cellulose are under investigation, including its addition as paper fillers [120], reinforcement in polymer composites [121], coatings for paper and board [122-125]

or stand-alone films [126,127]. However, the focus of this work is on the application of NFC as barrier material used in food packaging and printed electronics. High potential of NFC application as oxygen barrier material on the laboratory scale has already shown in several works [128-132].

There is a widespread desire and urgent need to replace or partially replace petroleum-based materials with renewable, biodegradable, and eco-friendly packaging materials. Furthermore, there are increasing interests focused on the performance of nanofibrillated cellulose-containing packaging materials regarding to the end-use properties, such as strength and barrier properties. However, the usage or application of hemicelluloses in packaging is currently limited.

Citric acid is easily accessible, inexpensive and a non-toxic food additive. It has been reported to be utilized as a cross-linking agent to improve the performance of starch, cellulose and PVA/starch films [133-135]. The barrier and mechanical properties of plasticized and cross-linked nanofibrillated cellulose coatings for paper packaging applications have been studied [136]. There has not been information reported using citric acid as a cross-linking agent in glucomannan/nanofibrillated cellulose composite films to enhance the moisture barrier and

mechanical properties. The purpose of this study was to formulate hemicellulose-based stand-alone films with improved moisture barrier and mechanical properties achieved by addition of citric acid as a crosslinking agent. The main focus was to explore the optimal film formulations in regard to the barrier and mechanical properties, which will prepare the films for future printing and packaging applications.

4.3 Experimental

Glucomannan from NOW Foods, Inc. in powder form was used. It was derived from the root of *Amorphophallus konjac* (Konjac plant or elephant yam). It is a glucose-mannose polysaccharide in which 5-10% of the sugars are acetylated. The molecule is structurally related to glucomannan from guar gum. Macroscopically, Konjac glucomannan is a soluble, fermentable, and highly viscous fiber.

Nanofibrillated cellulose, (NFC, contains: water 95%-99%, cellulose pulp 1-5%; manufactured by the Department of Chemical and Biological Engineering, University of Maine Process Development Center) in a suspension form, was employed in this study. The sample was prepared mechanically by using a pilot scale refiner to break down the wood fibers. The wood

fibers were a bleached softwood Kraft pulp. The suspensions were obtained at around 3.5% solids.

Sorbitol in powder form with a purity of 99%, from Sigma Aldrich, Citric Acid and Sodium Hypophosphite (SHP) from Sigma Aldrich in powder form with a purity of 98% were applied.

The composite film formulations are shown in Table 12. The nanofibrillated cellulose (NFC) was added to distilled water for 15 min (10 g/100 ml) with 0.5% glucomannan (w/w, on a NFC basis), 10% sorbitol (w/w, on a NFC basis), citric acid (5%, 15%, 25%, 35% w/w on a glucomannan basis), with SHP (50% w/w on a citric acid basis), by using a VWR Power Max ELITE Dual Speed Mixer at 45 °C and mixing speed of 450 RPM. The solutions were casted to a mold with the dimensions of 200 mm×100 mm. Films were dried in an Environmental Test Chambers (Caron Model 6010; temperature range: 5 °C to 70 °C; humidity range: 20% to 98% RH) for 24 hours at 60 °C and 35% relative humidity (RH). Dried hemicellulose-based films were peeled off manually and then subjected to a curing treatment at 105 °C for 10 min using a fan oven (VWR Model 1305 U). Three film series were prepared following the same procedures, namely, N-CA (films without citric acid), CA-C (those added with citric acid and cured) and

CA25-NC (added with 25% citric acid and not subjected to the curing treatment).

Table 12 The Crosslinking Film Formulations.

Component*	NFC	Glucomannan	Xylitol	Citric Acid	SHP**
N-CA	0.4	1	2	0	0
CA5-C	0.4	1	2	0.05	0.125

Table 12 - continued

CA15-C	0.4	1	2	0.15	0.125
CA25-C	0.4	1	2	0.25	0.125
CA35-C	0.4	1	2	0.35	0.125
CA25-NC	0.4	1	2	0.25	0.125

* All components are in grams

* *Sodium Hypophosphite as catalyst


Water vapor permeability of the films was evaluated by the gravimetric MVTR test according to the ASTM E96 desiccant method [137]. The samples were placed on top of a test cup (Thwing-Albert EZ-Cup 2”) containing sufficient amount of desiccant (anhydrous calcium chloride) to maintain 0% relative humidity, and the films were sealed to the cup (Figure 23). The assembled cups were placed in the testing room at 23°C and 50% RH and weighed every 24 h until constant rate of weight gain was attained. The MVTR were calculated by Eq. (4.1).

$$MVTR = \frac{G}{(A \times t)} \quad (4.1)$$

Where G is the weight change of the film, in grams; A is the area of the tested film, in cm²; t is

the time during which G occurred.

Table 13 MVTR Permeability Properties of Polypropylene and Other Plastics Films [138].

Film type		$\text{g/m}^2/\text{day}$
Biaxial-Oriented PP	Good MVTR	3.9-6.2
HDPE		4.7-7.8
Cast PP		9.3-11.0
Biax PET		16-23
LDPE		16-23
EVOH		22-124
OPS		109-155
Biax NYLON-6	Poor MVTR	155-202

The typical MVTR barrier values are shown in the Table 13 [138]. The water solubility test was conducted on the same specimens that were cut and used for the MVTR measurements. The specimen was a round piece with diameter of 2.5 inch. The film specimens were dried in the oven (VWR Scientific Model 1305 U) at 105 °C for 15 min and then weighed. Then the samples were immersed in 50 ml of distilled water for 6 h at 25 °C with continuous stirring using a magnetic stirrer (Corning Model PC-420). The remaining film pieces were dried and weighed. The insoluble matter was calculated as a percentage of the remaining weight over the initial weight of the film specimen.

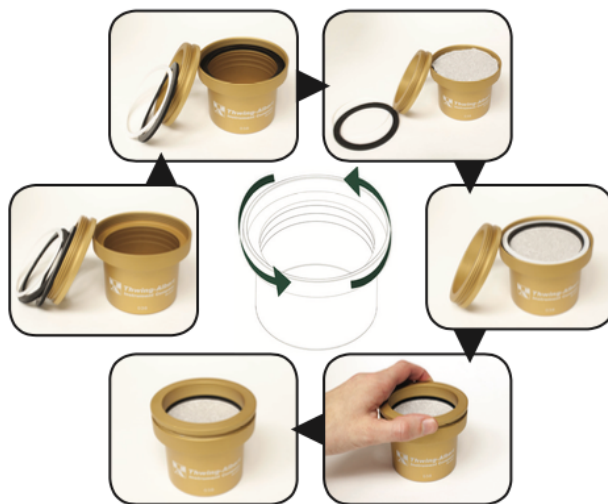


Figure 23 The Thwing-Albert EZ-Cup and Tested Films [138].

The tensile properties of the film samples were assessed according to TAPPI Standard T494 at 23 °C and 50% RH using an INSTRON 430I with a 500 N load cell. The specimens were conditioned under 23 °C and 50% RH for 24 hours prior to testing. The initial gauge length was 100 mm, and the crosshead speed was 25 mm/min. The width of each specimen was 15 mm. The average value and standard deviation of tensile strength, Young's modulus (E) and elongation at break were evaluated for at least 5 of the tested specimens.

The surface energy of the films (CA25-C, CA25-NC and N-CA) was estimated by the FTA200 (First Ten Angstrom Dynamic Contact Angle) measurement apparatus. The FTA200 is a flexible video system for measuring contact angle, surface and interfacial tensions, wettability, and

absorption. For the evaluation of the surface energy, the contact angle of three liquids, deionized ultra-filtered water (DI), hexadecane, and methylene iodide (MI), were measured against surfaces of the N-CA and CA-C film series, and the critical surface energy was calculated using the Owens-Wendt [65] method as well as by the Good-Girifalco [140] Young-Dupre equation [62]. Although these methods only estimate the solid surface energy, such values are useful for comparing the wettability of solid surfaces and predicting print adhesion. During each measurement, a droplet of liquid (1 μ L) was deposited on the film specimen surface through a needle with 0.7 mm diameter. A series of images were captured and analyzed. A minimum of 5 readings were taken for each sample.

4.4 Results and Discussion

4.4.1 Caliper

The caliper of the film samples was measured by the Technidyne PROFILE/Plus Thickness instrument. The calipers of the film samples are shown in Table 14. The importance to characterize the caliper of the sample films is to ensure the repeatability of the film formation procedures in regard to caliper as well as to eliminate the impact of varying caliper on the barrier

properties of the film samples. Thus, consistent caliper will enable to compare film series with various formulations and verify the crosslinking effectiveness. The film caliper was controlled by utilizing equal mass of hemicellulose-based film suspension to fill the casting mold with identical dimensions.

Table 14 The Caliper of Hemicellulose-based Films.

Sample	Caliper/mm
N-CA	0.36±0.01
CA5-C	0.35±0.01
CA15-C	0.38±0.03
CA25-C	0.37±0.02
CA35-C	0.37±0.02
CA25-NC	0.36±0.01

4.4.2 Moisture Vapor Transmission Rate (MVTR)

The moisture vapor transmission rate (MVTR) of the films characterize the volume of water vapor passing through a film per unit area and time under specified conditions. MVTR was measured at a steady state following ASTM E96 standard. The expectation for the CA-C films is lower MVTR and higher strength. The water vapor transfer rate for a packaging material such as LDPE (low density polyethylene) is 16- 23 g m⁻² day⁻¹ for film with 1 mm thickness [138]. In

this study, the CA-C film series fulfilled this requirement. The N-CA films also fulfilled this requirement, but hornification occurred and resulted in higher opacity and rougher surface, which could lead to poor printability.

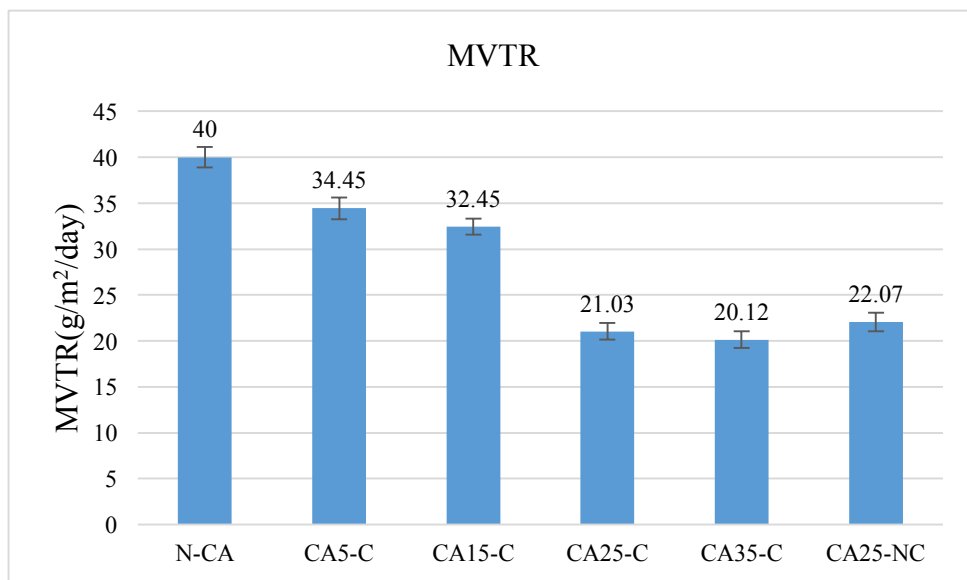


Figure 24 The Moisture Vapor Transmission Rate for the Hemicellulose-based Films.

The values (Figure 24) show a reduction of MVTR with addition of citric acid. The MVTR tended to decrease with the addition of citric acid. The fall of MVTR values may be caused by a decreased solubility of water in the amorphous regions of the hemicellulose structure as an increasing fraction of the acetylated hydroxyl groups, or simply more thorough crosslinking.

The relatively low air permeability of the films indicates that there were few connected pores through the cross section of the films. Therefore, it would be of interest to investigate the oxygen

transmission rate (OTR) in the future work of this study since it is a very important property for food packaging materials. The gas permeability depends on the dissolution of oxygen and its rate of diffusion in the material when there are no pores allowing for gas to flow through it.

4.4.3 Tensile Properties

Tensile properties for the different film series are presented in Table 15. Some studies have reported that citric acid not only effects moisture barrier properties of polysaccharide films, but also functions as a plasticizer to improve their tensile properties [140]. Correspondingly, this study presented that these effects apparently coexist. On one hand, citric acid addition decreased the MVTR and soluble matter of the films by approximately 13%, indicating the crosslinking reaction between glucomannan and citric acid. On the other hand, the tensile strength, modulus and elongation at break increased with addition of citric acid, reflecting a functioning of citric acid as plasticizer. According to the study of Wang et al. [141], the plasticizing effect of citric acid was attributed to increasing interstitial volume of the film or increasing molecular mobility, making the polymeric structure less dense. However, over cross-linked (CA35-C) hemicellulose is brittle and lacks elasticity.

Table 15 The Tensile Properties of the Hemicellulose-based Films.

Sample	N-CA	CA5-C	CA15-C	CA25-C	CA35-C
Tensile Strength (N/m ²)	2.49±0.11	2.47±0.22	2.89±0.25	3.47±0.12	2.98±0.11
Modulus (N/m ²)	0.011±0.002	0.013±0.001	0.013±0.001	0.016±0.001	0.013±0.002
Elongation (%)	23.38±1.20	22.12±2.10	23.31±2.30	25.55±1.80	22.50±1.30

4.4.4 Surface Energy

When it comes to printing, it is essential to understand the behavior of ink on the chosen substrate. Surface energy/tension is responsible for the surface behavior (atmosphere-solid contact) and the wetting phenomena (liquid-solid contact).

Estimated surface free energy value of the CA25-C film surface is 40.92 mJ/m², while the surface tension of the silver conductive ink is 27-30 mJ/m² (Table 16). This product has good wetting with ink and high ink adhesion on the N-CA film surface. Hemicellulose is hydrophilic in nature, hence hemicellulose-based films are generally hygroscopic, which means they will absorb moisture. During the surface free energy estimation test, the water drops spread on the films and totally wet the surface. However, the methylene iodide drops bead up on the film surface. This is because the hemicellulose has abundant free hydroxyl groups distributed along

the main and side chains and is affinitive to water.

Table 16 The Surface Energy Estimation of the Film Surfaces.

Sample	Surface Energy (mJ/m ²)	Dispersive (mJ/m ²)	Polar (mJ/m ²)
N-CA	64.96	20.18	44.78
CA25-NC	42.65	35.43	7.22
CA25-C	40.92	38.78	2.14

4.4.5 Solubility

The solubility and the degree of swelling are very important properties for food packaging. The solubility usually decreases as the degree of crosslinking increases [142]. The solubility values of the N-CA, CA-NC and CA#-C films are found in the Table 17. The CA-NC film has lower solubility than the N-CA film samples, while there is no significant difference of solubility between the CA-NC and CA#-C film samples. This indicates the crosslinking may happen during the mixing and drying process even without film curing. The CA#-C and CA-NC films result in lower solubility, which corresponds to their lower MVTR values.

Table 17 The Solubility Values of the Film Series.

Sample	N-CA	CA5-C	CA15-C	CA25-C	CA35-C	CA-NC
Initial Weight (g)	1.02	1.05	1.05	1.04	1.03	1.02
Dry Weight (g)	0.36	0.39	0.44	0.51	0.56	0.49

Solubility %	64.20	62.85	58.09	51.14	45.63	51.96
--------------	-------	-------	-------	-------	-------	-------

4.5 Conclusions

In summary, the glucomannan/NFC stand-alone films were successfully formulated from the solution through mixing, followed by film casting in the presence of citric acid. The addition of citric acid led to a significant enhancement in moisture barrier properties. Citric acid was shown to be effective as a cross-linker, and it decreased water solubility and water vapor permeability of innovatively formulated glucomannan/NFC composite films. Citric acid also functions as a plasticizer to increase the tensile properties of the hemicellulose-based films, proved by higher tensile strength and elongation. Moreover, the crosslinked glucomannan film resulted in a lower solubility. Due to the biodegradability and biocompatibility, this biopolymer film based on glucomannan nanofibrillated cellulose with improved moisture barrier properties possess potential in food packaging and offers an alternative to petroleum derived products. This work was done in laboratory scale, and therefore more experiments need to be done to scale up stand-alone films production into industrial settings.

CHAPTER 5

SCREEN PRINTED MOISTURE SENSOR ON HEMICELLULOSE-BASED BARRIER COATED SBS BOARD

5.1 Abstract

The hemicellulose with nanofibrillated cellulose (NFC) composite films exhibit outstanding air barrier properties, which supports their applications as bio-based and biodegradable barrier coating on food packaging materials. The hydrophobic property of the hemicellulose-based biopolymer has been greatly improved (MVTR decreased by 49.7%) with crosslinking by using citric acid. In this work, the crosslinked bio-polymer suspension was applied on back side of solid bleached sulphate (SBS) board with a Meyer rod. Interdigitated electrodes were designed as moisture sensors and then screen printed on the back side barrier coated SBS board with silver conductive ink. The hemicellulose-based barrier coating layer functioned as a moisture sensing layer. The printed sensor device was calibrated with its absorption and desorption isotherms at 23 °C with the range of relative humidity 20%-80%, followed by characterizations of the sensor's impedance change with each moisture level ranging from RH 20% to 80%. The breakthrough time was observed for each level of RH by measuring impedance using the LCR meter. These

findings point to the opportunity of coupling the hemicellulose-based barrier coatings with printed moisture sensor in order to boost their capabilities as smart barrier packaging materials.

5.2 Introduction

Flexible polymers are widely used in a multitude of food packaging applications, ranging from potato chips to take-away food wrappings. The current packaging industry strongly relies on petroleum-derived barrier films with production processes contributing to the emission of greenhouse gases. Moreover, a majority of consumer packages go to landfill after a short usage life, which leads to environmental issues and sustainability limitations.

Polysaccharides that are used for packaging are chitosan, starches, cellulose and hemicellulose. They are nontoxic, widely used and available in the market, and abundant also as waste materials. With great gas, aroma and grease barrier properties, such coatings have great potential in packaging industry. However, because of their hydrophilic nature, polysaccharides exhibit poor water vapor barriers [143,144].

Barrier coating layers for paper and board are commonly applied as dispersions or solutions. In the case of hemicellulose-based barrier coatings, the preparation of the dispersions often requires

the use of citric acid to crosslink the polymer chains in order to form a three-dimensional network, which will improve the water resistance of the coating.

Porous cellulose-based materials, such as paperboard, have a great impact in the packaging industry due to their eco-friendly nature and biodegradability. However, hydrophilic behavior and porous structure has limited the use of paper in a wide range of packaging applications. In order to overcome this issue, paper or paperboard is usually coated with a polymer or metal layer such as plastic or aluminum, to provide improvements in barrier properties at the expense of their eco-friendly and biodegradable nature [145].

Therefore, researchers are working to improve the moisture barrier property of the polysaccharides in order to broaden their potential applications on packaging materials. One way to increase the flexibility of the hemicellulose coating is to reduce the number of hydrogen bonds using plasticizers, such as sorbitol [146] or glycerol [147,148]. These plasticizers have been shown to increase the tensile strength [149,150] and the oxygen barrier of films.

Another method to improve the dimensional stability and increase the hydrophobicity of coatings is through chemical crosslinking (e.g. esterification). The cross-linking procedure consists of the

functional modification of the NC without its disintegration [151]. Different chemicals, such as toluenesulfonic acid, hexanoic acid [152], butyryl, benzoyl, naphthoyl, diphenyl acetyl, and stearoyl [153] have been used to carry out this chemical crosslinking procedure. However, poly (carboxylic acids) such as citric acid [154] or succinic acid [155] have become very popular because of their environmentally friendly and non-toxic nature. The cross-linking technique has also been used to improve the wet strength of cellulosic materials and to decrease the solubility of polysaccharides in water [156].

In our earlier study, barrier films based on hemicellulose, NFC and plasticizers were formulated [114]. Their mechanical strength (tensile properties), surface properties (contact angle, surface energy, and PPS roughness) and printability (print density) were characterized. Then the strongest formulation of the stand-alone film was chosen to be crosslinked with citric acid in order to improve strength and barrier properties. We evaluated the air permeability and water vapor transmission rate of the crosslinkable films against several benchmarks [157]. It was observed that given the same thickness of films, the MVTR, tensile properties and insoluble matter of the crosslinked formulations surpassed the film formulations without citric acid

crosslinking. These positive results encouraged the further development of crosslinkable glucomannan-based barrier coating formulations with respect to their industrial applications in roll-to-roll coating processes and smart packaging applications with printed electronics.

In this study, the barrier coating mixtures were formulated based on the crosslinked formulation of the hemicellulose-based film. An aqueous suspension of the barrier coating was prepared. The most promising formulations were coated onto back side of commercial SBS board with Meyer rod, and the water vapor transmission rate (WVTR) and air permeability were characterized.

It is known in the food industry that a large amount of food is wasted during the transportation chain each year. Accurate monitoring and controlling of the environmental conditions imposed on perishable goods throughout transportation could optimize the transportation chain, yielding reduced waste. Currently, it is already possible to envisage new applications related with smart packaging for perishable goods through printed electronics. Due to their potential low cost per surface area, mechanical flexibility and possibility of large scale processing [158,159], printed electronics encourage new opportunities in the field of sensing and electronics such as distributed sensing applications at large scale or monitoring of a high number of items in parallel.

Research in humidity capacitive-based sensors on plastic films has been reported [75,76,160]. An important part of these sensors utilizes the ability of certain polymers to absorb humidity, which will modify their dielectric properties. A type of micro sensor has been developed using gold patterned on parylene, and polyimide as the sensing layer [161]. Polyimide has also been used as substrate material for ultra-thin flexible chemical capacitive sensors in 2009 [162].

Resistive type humidity sensors contain noble/precious metal electrodes either deposited on a glass or ceramic substrate by thick film printing techniques [163] or thick film deposition [164].

The design configuration of most resistive sensors is based on interdigitated electrodes [75,76,165] in which the humidity sensitive films are deposited in between them such that they touch the electrodes. The platform substrate can be coated either with electrolytic conductive polymers, such as salts and acids [166, 167] or doped ceramic sensing films [168, 169]. In some cases, the film-based sensors are formed by applying screen printing and coating techniques such as spin coating and dip coating.

Resistive sensors measure the change of the humidity and translate it into a change in electrical impedance of the hygroscopic medium. Typically, the change of resistance to humidity follows

an inverse exponential association, and almost varies from 1 K Ω to 100 M Ω . As a principle, upon adsorption of water vapor its molecules are dissociated to ionic functional hydroxyl groups and this results in an increase of film electrical conductance.

In this study, the hemicellulose-based barrier coating was applied on to back side of the commercial SBS board, and on top of it was screen printed moisture sensor. The devices that can sense the moisture change are interdigitated electrodes capacitors as depicted in Figure 25 (a). It allows direct interaction between the sensor and the surrounding atmosphere. The primary design of the electrode capacitors included 20 pairs of planar electrodes of 7 mm length each, occupying a total surface area of 10mm \times 4mm.

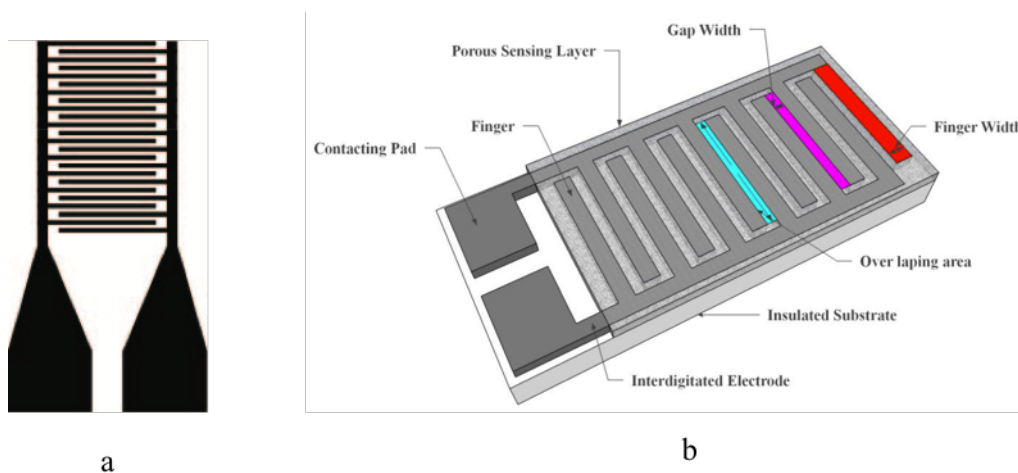


Figure 25 The Design Interdigitated Electrode (a) and Its Detailed Structure (b) [170].

The moisture sensor principle is based on the ability of certain structures to shift its capacitance and resistance in the presence of a target humidity level [171]. The interdigitated electrodes capacitors generate an electric field in both the dielectric layers underneath and on top of the electrodes plane. The layer underneath the electrodes will be referred as the substrate of the device. In this study, the substrate is back side of SBS board which provides mechanical support.

The hemicellulose-based barrier coating that functions to absorb the moisture vapor is called the sensing layer.

The water vapor is ideally adsorbed and desorbed in the coating layer. As a result, the sensing layer swells (increasing thickness) and its dielectric constant ϵ changes, modifying the value of capacitance. The thicker the sensing layer is, the larger the amount of water molecules it can absorb under a fixed humidity level.

The aim of this study is to develop flexible packaging films [114] and coatings that are based on biodegradable, biocompatible and recyclable materials including nanofibrillated cellulose and glucomannan. These films and coatings are aiming to provide competitive barrier properties and ultimately leading to repulpable and biodegradable materials for packaging applications.

5.3 Experimental

5.3.1 Materials

Glucomannan from NOW Foods, Inc. in powder form was used. It was derived from the root of *Amorphophallus konjac* (Konjac plant). It is a glucose-mannose polysaccharide in which 5-10% of the sugars are acetylated. The molecule is structurally related to glucomannan from guar gum. Macroscopically, Konjac glucomannan is a soluble, fermentable, and highly viscous fiber.

Nanofibrillated cellulose, (NFC, contains: water 95%-99%, cellulose pulp 1-5%; manufactured by the Department of Chemical and Biological Engineering, University of Maine Process Development Center) in a suspension form, was employed in this study. The sample was prepared mechanically by using a pilot scale refiner to break down the wood fibers. The wood fibers were a bleached softwood Kraft pulp. The suspensions were obtained at around 6.5% solids.

Sorbitol in powder form with a purity of 99%, from Sigma Aldrich was used. Citric Acid and Sodium Hypophosphite (SHP) from Sigma Aldrich in powder form with a purity of 98% were

employed.

5.3.2 Coating Formulation

The hemicellulose-based barrier coatings are formulated based on the best stand-alone film formulation (CA25-C) in terms of their barrier property against moisture (characterized by MVTR), found in our previous research. [157]

Table 18 The Crosslinking Barrier Coating Formulation.

Component	NFC	Glucomannan	Xylitol	Citric	SHP*
[g]	[g]	[g]	[g]	Acid [g]	[g]
CA25-C	0.4	1	2	0.25	0.125

*Sodium Hypophosphite as catalyst

The prepared dispersion was coated on the back side of 266 g/m² SBS board on a laboratory scale. The coating was performed with a Meyer rod #46 that is capable of producing a 11.6 mm wet film thickness. The coated board samples were dried in the standard conditioning laboratory with 23 °C, RH 50% for 24 hours. The coating and drying processes were repeated 5 times in order to get significantly improved barrier properties. The barrier property was characterized by MVTR using the gravimetric method according to the ASTM E96 desiccant method [137].

5.3.3 Calendering and Conditioning of Samples

The coated samples were calendered at pressure of 25 psi, 2-nip smooth side. The PPS roughness of the calendered samples was under 3 microns. All calendered samples were conditioned for 24 hours at 50% RH and 25 °C before any measurements were made.

5.3.4 Sensor Printing

The interdigitated electrodes were printed on the hemicellulose-based barrier coated SBS board by using a precise screen printer (MSP-485 Affiliated Manufacturing Inc.) with silver conductive ink (AG-800 Applied Ink Solution). A stainless steel screen, fabricated at Microscreen[®] with 325 mesh count, wire diameter of 28 μm , mesh angle of 22.5°[172]. The printed electrodes have an initial resistance of $18.5 \pm 0.6 \text{ M}\Omega$ due to poorly connected silver particles, and resistance decreased through sintering, which is a process that enhances junctions among particles and reduces resistivity. High temperatures can, for example, cause sintering by evaporating solvent and binders which cause neck formation and particle growth that reduces a printed electrode's resistivity. The printed sensors were placed in an oven at 130 °C for 5 min in a VWR 1320

temperature controlled oven to thermally cure and sinter the conductive ink.

5.3.5 Sensor Testing

The response of the impedance sensors was tested against changes in the humidity level from 20% to 80% RH at a constant temperature of 25 °C. For this purpose, the printed moisture sensors were placed in the conditioning laboratory for 24 hours at 25 °C and 50% RH. An uncoated SBS board was also conditioned and tested as control sample. Then the devices were put in a Thermotron[®] SE 1000 environmental chamber, which allowed for the automatic control of wet and dry airflow inside the cell at various temperature of choice. The chamber is equipped with an 8800 Data Acquisition (DAQ) system for controlling, monitoring, graphing and reporting environmental chamber data. The printed electrode was connected to an LCR meter (Agilent E4980a Precision) through wires and was put in the chamber with 20% RH without any sealed desiccant cup. The LCR meter was controlled by a custom-built LabVIEW[™] program on the PC and used to record the impedance response of the printed sensor at an operating frequency of 1 kHz and an applied voltage of 1 V (Figure 26). The LCR-meter was used to measure the corresponding impedance values at a frequency of 1 kHz after the relative humidity and

temperature reached stable values. Impedance and time measurements were controlled and recorded through a PC. Post-measurements data treatments were carried out with a PC to obtain differential values of impedance. This testing process served to equilibrate both sides of the sensor with moisture, providing a reliable base point that can be compared with the uncoated SBS board, hence evaluate the barrier property of the coated SBS board. When observed the impedance reaching a constant level, it indicates that the sample has reached an equilibrium. Then the humidity level was increased from 20% RH to 80% RH with 10% increasing intervals until seven basepoints were observed and collected.

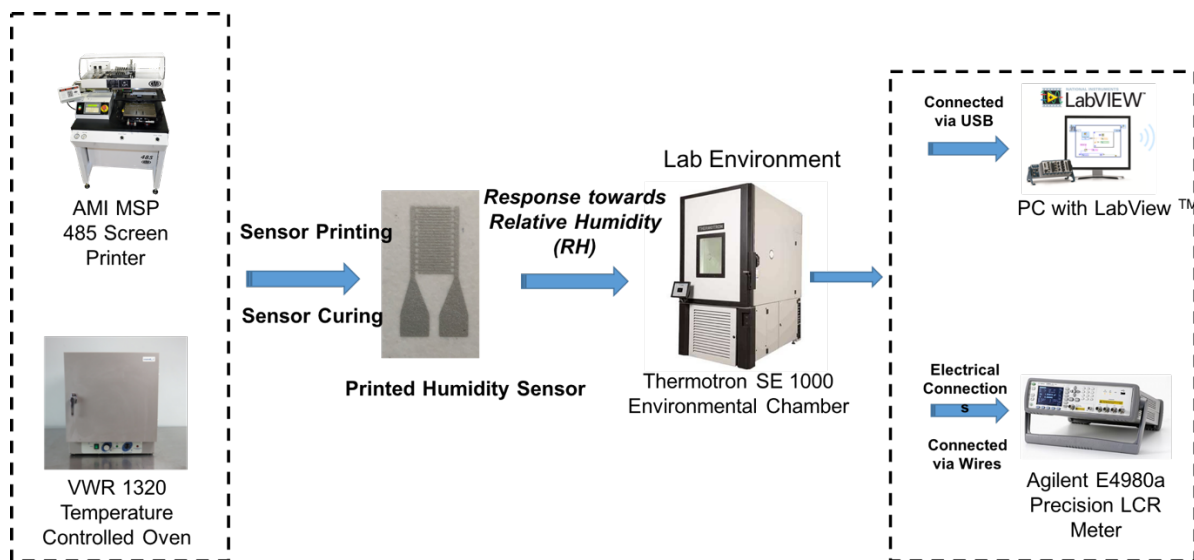


Figure 26 The Experiment Setup for the IDE Humidity Sensor Printing and Characterizations.

5.4 Result and Discussion

The objective of the sensor testing conducted in the humidity chamber was to identify if the hemicellulose-based coating layer on the SBS board is efficient to function as a barrier layer against moisture, hence be capable of being applied to food packaging materials for future use and further research development.

5.4.1 Barrier Properties Analysis

The barrier properties of the hemicellulose-based coated SBS board were characterized by correlating its coating thickness and coat weight versus its air permeability and MVTR (Table 19). The coating formulation was chosen according to the best stand-alone film formulation in regards to its MVTR value. The coated SBS board has a decreased air permeability coefficient by 2 orders of magnitude. Meanwhile, the barrier property characterized by moisture vapor transmission rate (MVTR) of the coated SBS board has been improved by 81.5%. Both the coat weight and coating thickness can be tuned by varying coating method, such as Meyer rods, depending on the end-use or application of the coated SBS board.

Table 19 Barrier Properties of the Hemicellulose-based Coated Board.

Sample	Caliper/ mm	Coating Thickness/ μm	Air Permeability Coefficient/ μm^2	MVTR/ $\text{g}/\text{m}^2\text{day}$	Coat Weight/ g/m^2
SBS	0.353	n/a	5.39×10^{-3}	213.0	0
CA-C	0.371	18	4.07×10^{-5}	39.4	14.9

5.4.2 Humidity Sensor Response Analysis

The impedance humidity measurements were made in a humidity chamber (Thermotron[®] SE 1000) at a fixed temperature of 25 °C. The printed sensors on both coated and uncoated SBS boards were tested under a wide humidity range from 20% to 80% RH in 2 hour intervals. The humidity levels were set up in this interval due to the physical constraints of the humidity chamber. The selected time period was set up to 2 hours in order to allow the diffusion of water vapor molecules to be absorbed into the substrate and stabilized, reaching the equilibrium with the environment.

The output signals of both sensors were normalized to the nominal values of capacitance C_0 and resistance R_0 . The real and the imaginary part of the sensor impedance are recorded during step-wise changes between 20% to 80% RH in 2 hour intervals. Stable humidity conditions are

typically achieved within less than 15 minutes. The humidity equilibrates to stable levels with a small remaining drift (Figure 27). The real Z' and imaginary Z'' of the complex paper-based sensor impedance ($Z = Z' + iZ''$, where $i = \sqrt{-1}$) is recorded with test frequency of 1 kHz.

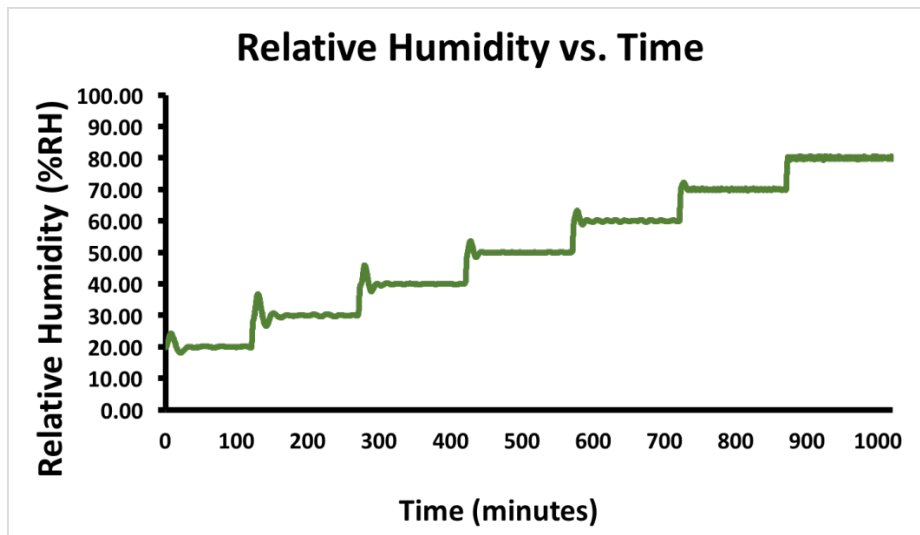


Figure 27 The Stepwise Change of the Relative Humidity in the Test Chamber.

Figure 28 shows the dynamic capacitance response of the sensor printed on the uncoated SBS board. The capacitance of the sensor printed on uncoated SBS board stepwise increased, corresponding with the increasing relative humidity in the chamber.

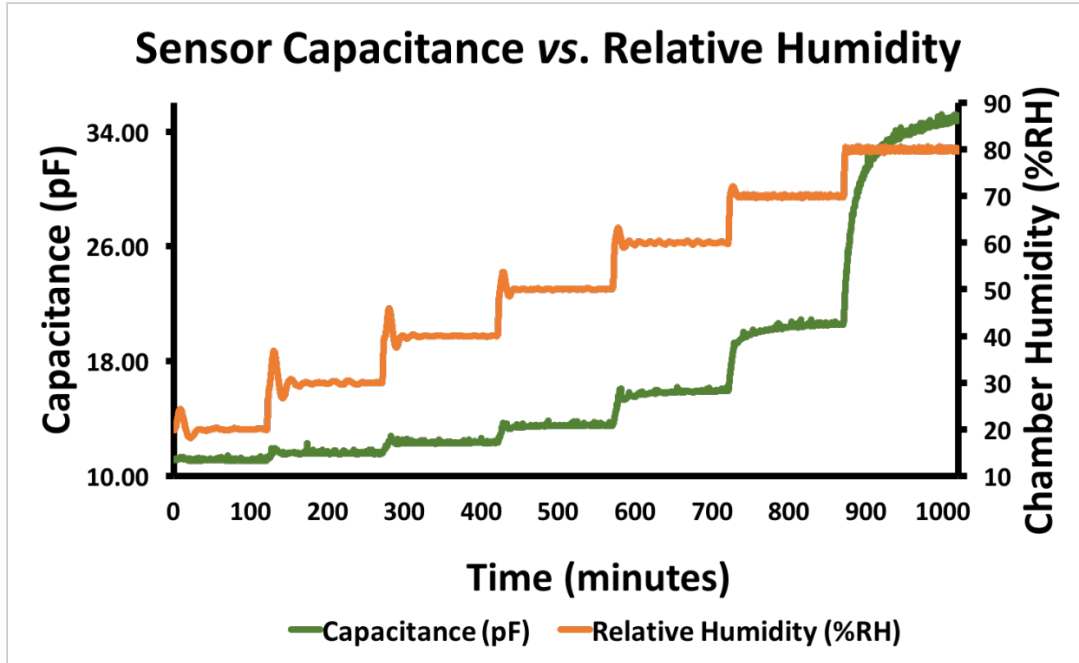


Figure 28 Capacitance vs. RH Plot of Sensor Printed on Uncoated SBS Board.

Figure 29 shows the dynamic capacitance response of sensor printed on the coated SBS board.

The behavior shows a delaying of the sensor in the increasing RH intervals. This is due to saturation of the barrier coating functions as the sensing material. It can be explained by the adsorption process for the sensor when exposed to different relative humidity levels. The capacitance of the sensor printed on coated SBS board remains stable before the relative humidity in the chamber reached 75%. This behavior indicates the barrier coating layer successfully block out the moisture and delay the water vapor break through before 75% RH. Moreover, it can be observed from Figure 29 that at 80% RH, the capacitance of sensor printed

on coated SBS board didn't reach equilibrium within the 2-hour interval. This indicates that at 80% RH, it will take more than 2 hours for the moisture vapor to break through the hemicellulose-barrier coating layer. In other words, the barrier property of the coating layer is shown to be significantly effective.

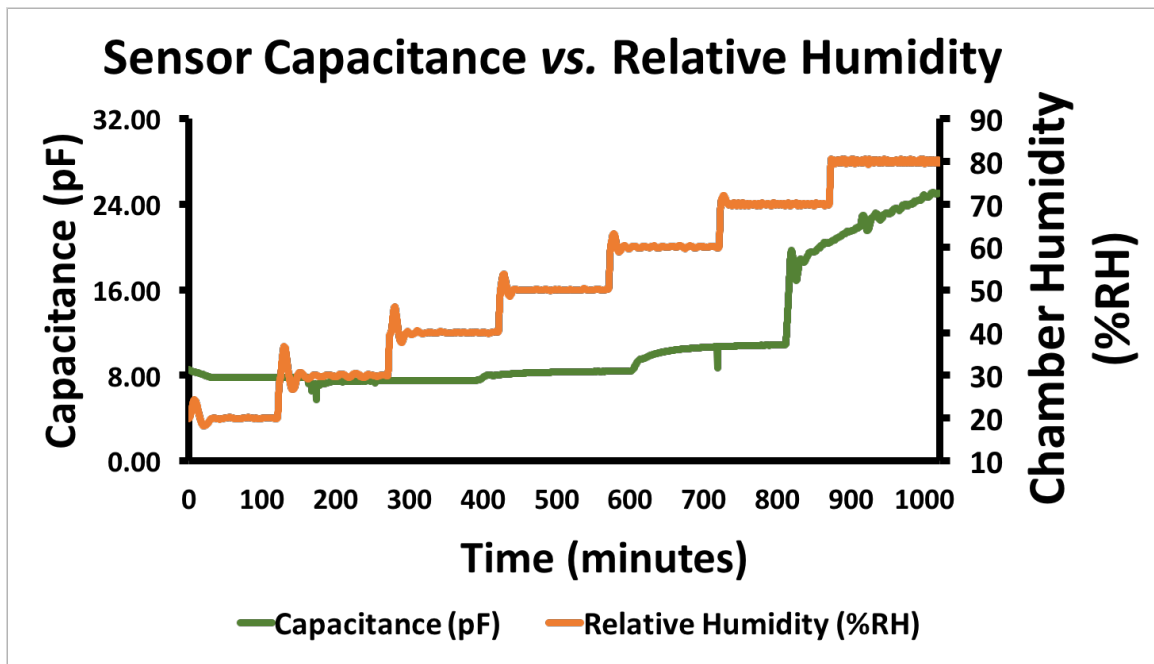


Figure 29 Capacitance vs. RH Plot of Sensor Printed on Coated SBS Board.

From the measurement data (capacitance and conductance) we are able to derive the sensor impedance using the equation (5.1)

$$R_x = \frac{1}{G_x}; \quad Z = \frac{R_x}{1 + j\omega R_x C_x} \quad (5.1)$$

Where,

ω is the angular frequency;

$$\omega=2\pi f; f=1 \text{ kHz.}$$

The resistance on the coated SBS board also shows a delaying response (Figure 30), while for the uncoated SBS board, the resistance increases in stepwise correspondently with the increasing RH without hysteresis response (Figure 31).

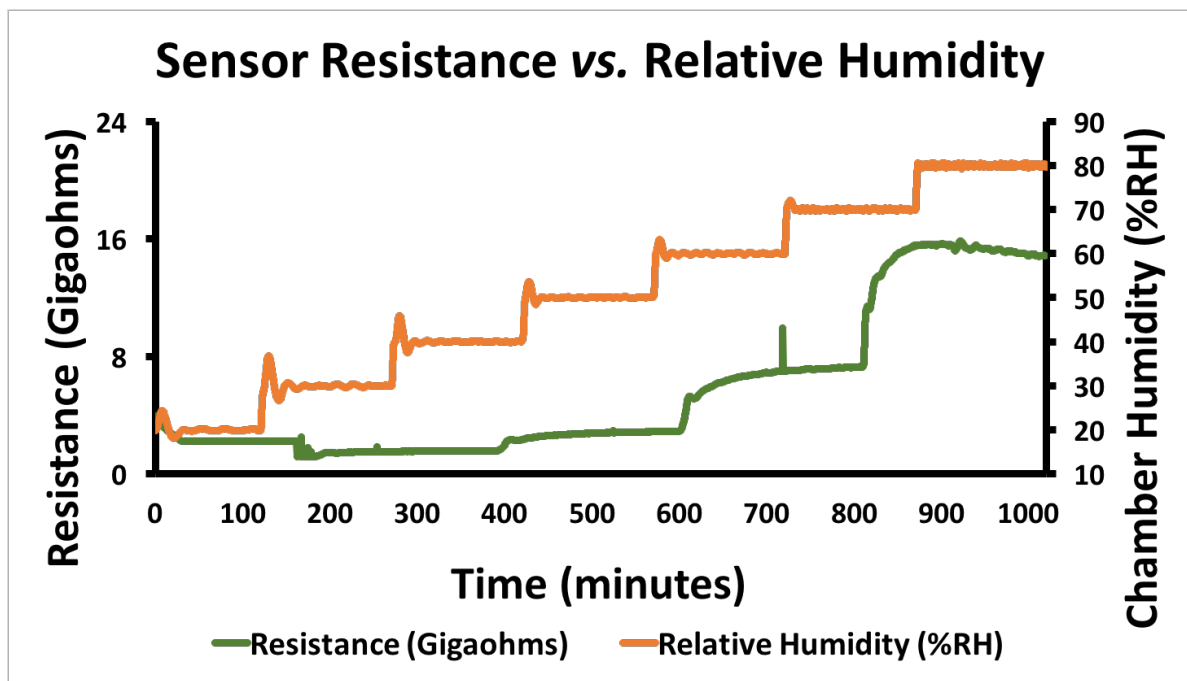


Figure 30 Resistance vs. RH Plot of Sensor Printed on Coated SBS Board.

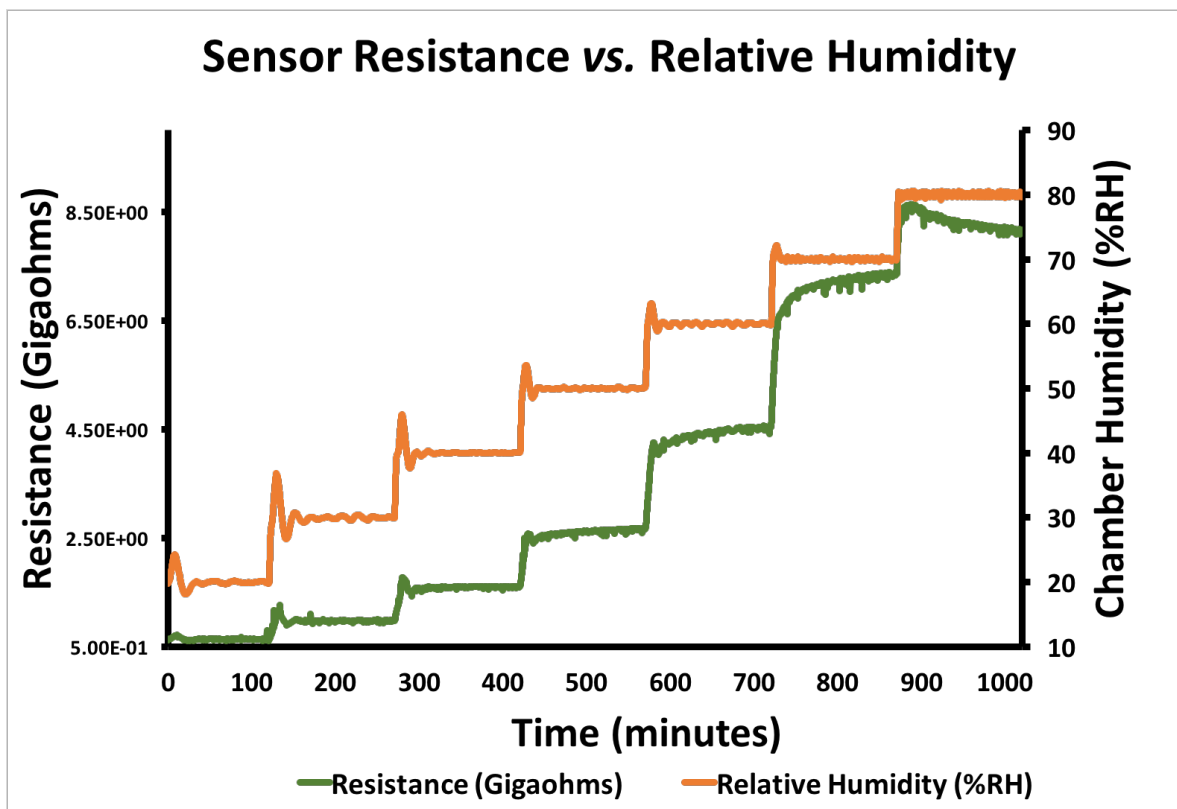


Figure 31 Resistance vs. RH Plot of Sensor Printed on Uncoated SBS Board.

In Figure 30 we can observe non-linear response of sensor printed on the hemicellulose-based barrier coated SBS board. It is very obvious that the resistance of the printed sensor remains stable around 3 Gohms from 20% to 50% RH. When the RH increased to 75%, resistance has a breakthrough of 16 Gohms, indicating the dielectric constant of the coated SBS board was changed due to the total saturation of moisture vapor. In comparison, from Figure 31 we can observe the resistance response of the sensor printed on the uncoated SBS board increased stepwise with the increasing RH levels. Without any barrier coating, there is no delay in

response.

5.5 Conclusion

A hemicellulose-based barrier coating was formulated and applied onto SBS board successfully.

The barrier property has been characterized with its air permeability and moisture vapor transmission rate. A screen printed impedance humidity sensor was successfully designed, fabricated and tested. Tests were conducted in a humidity chamber by varying the relative humidity levels and measuring the changes in impedance. One of the objectives of this study-to develop a moisture and air barrier coating that can be applied in food packaging, has been fulfilled. Also, the impedance sensor printed on the coated and uncoated SBS boards has been analyzed at various RH levels. The impedance of the sensor increases with the increasing RH levels. However, the sensor printed on hemicellulose-based barrier coated SBS board delays the impedance increase until the RH reached 75%. This indicates that the hemicellulose-based barrier coating functions efficiently to block the moisture under low to moderate RH, hence possesses the potential to serve as liquid detector in moisture surveillance and tracking functions along the transportation and storage process.

CHAPTER 6

CONCLUSION AND FUTURE WORK

The results and findings of this work advanced the understanding of the properties and applications of hemicellulose-based biofilm and barrier coating. In the first paper presented, the biofilm formulations were investigated by using the full factorial design of experiment using ANOVA. The main factors that significantly affect the film formation and film properties were analyzed. In order to explore the potential printing and packaging applications of the hemicellulose-based film, their mechanical properties (tensile and bursting strength), surface properties (surface free energy and PPS roughness) and printability tests were performed. The hemicellulose-based biofilm shows good capability in terms of its mechanical strength and printability to be applied as packaging material. However, due to the hydrophilic property of hemicellulose and nanofibrillated cellulose, the moisture barrier property limits the usage of the hemicellulose-based biofilm on packaging applications.

Therefore, as the second paper presented, the moisture barrier property of the hemicellulose-based film has been significantly improved through crosslinking with citric acid. The moisture barrier property of the film was characterized by the moisture vapor transmission rate (MVTR)

and it shows a significant decrease of 49.7%. Meanwhile, the mechanical strength has also been slightly improved with the citric acid functioning as plasticizer.

Having developed formulations of hemicellulose-based biofilms with significantly improved moisture barrier properties, further works were performed to develop a barrier coating formulation, as well as fabricate a printed moisture sensor on the hemicellulose-based barrier coated SBS board. The correlation of sensor impedance, relative humidity and time has been plotted. It was found that compared to the sensor printed on uncoated SBS board, the sensor printed on barrier coated SBS board has a significant delay of impedance increase with the increasing RH. This behavior shows that the hemicellulose-based barrier coating is capable of blocking out the moisture vapor and can be potentially used for packaging applications.

Future work should focus on the rheology analysis of the film suspension, aiming to develop the roll-to-roll coating and print trials to work through the process requirements for manufacturing thin printed and unprinted hemicellulose-based films. Moreover, it would be interesting to study the correlations of impedance printed humidity sensors versus relative humidity with varying RH and temperature. Characterizations of the humidity sensor sensitivity could be performed by

investigating the sensors' response time to varying RH levels.

6.1 Contribution to General Science

By providing a well-designed formulation of hemicellulose-based biofilm with improved moisture barrier property, as well as the surface property, mechanical property, solubility and printability, this work has contributed to the advancement of hemicellulose and nanofibrillated cellulose applications in fabricating biocompatible and biodegradable packaging materials. Furthermore, this work provides a good understanding of the hemicellulose-based barrier coating's interaction with conductive inks and printed electronics.

6.2 Contribution to Development of Practical Applications

Sensor applications are increasing in importance since products are required to become more intelligent and safe. In this study, hemicellulose-based barrier coatings were developed and proved to be efficient in moisture barrier property. The humidity sensor printed on hemicellulose-based barrier coated SBS board provides a practical solution for smart packaging that enables adding surveillance functions to ensure a better transparency and traceability.

In specific, the moisture breakthrough for coated SBS board are associated with an effective blocking mechanism. The robust performance of this sensor printed on hemicellulose-based barrier coated SBS board suggests potential applications as smart packaging with moisture surveillance functions or liquid detector in medical and sanitary products.

For example, the printed sensor can be applied to chip bags, to trace the humidity level changes along the storage and transportation process, providing surveillance functions to ensure that the food quality is preserved.

REFERENCES

1. Matthews, J. F., et al., *Computer simulation studies of microcrystalline cellulose I*. Carbohydrate Research, 2006. **341**(1), p. 138-152.
2. Gigli, M., et al., *Novel eco-friendly random co-polyesters of poly (butylene succinate) containing ether-linkages*. Reactive and Functional Polymers, 2012. **72**(5), p. 303-310.
3. Gu, J.-D., *Microbiological deterioration and degradation of synthetic polymeric materials: Recent research advances*. International Biodeterioration and Biodegradation, 2003. **52**(2), p. 69-91.
4. Shah, A. A., Hasan, F., Hameed, A. and Ahmed, S. *Biological degradation of plastics: A comprehensive review*. Biotechnology Advances, 2008. **26**(3), p. 246-265.
5. Kirwan M. J., *Food Packaging Technology (Book)*. Wiley, John & Son, Incorporated, 2003. P. 224-256.
6. Lehtinen E., *Papermaking Science and Technology: Pigment Coating and Surface Sizing of Paper*. Finnish Paper Engineers Association and TAPPI, 2000.
7. Lee, H. K., Joyce, M. K., and Fleming, P. D., *Influence of Pigment Particle Size and Pigment Ratio on Printability of Glossy Inkjet Paper Coatings*. Journal of Imaging Science and Technology, 2005. **49**:1, p. 54-61.
8. J. Kline, *Paper and Paperboard (Book)*, 2nd Ed., Miller Freeman Publishing, 1991. p. 245-260
9. Kuusipalo J., *Characterization and Converting of Dispersion and Extrusion Coated-HD-Papers*. TAPPI proceedings, 2003.
10. Washburn E. W., *The Dynamics of Capillary Flow*. Physics Review, 1921. **17**: p. 273
11. Halle, R. W. and Simpson, D. M., *A New Enhanced Polyethylene for Extrusion Coating and Laminating*. TAPPI Proceedings, 2003.
12. Alexander Kamyshny, Joachim Steinke, and S. Magdassi, *Metal-based Inkjet Inks for printed electronics*. The Open Access Applied Physics, 2011. **4**: p. 19-36.
13. Street R.A., *Jet Printing Flexible Displays*. Materials Today, 2006. **9** (4): p.32-37.

14. Trajkovikj J., et al., *Soft and Flexible Antennas on Permittivity Adjustable PDMS Substrates*. Loughborough Antennas and Propagation Conference. 2012, IEEE: Loughborough, UK. p. 1-4.
15. Compute Scotland, *Printed thin film transistor & memory*, 01/17/13, downloaded from www.computescotland.com/printed-thin-film-transistors-memory-5781.php, 07/7/18.
16. Dan Soltman, et al., *Screen printed resonant tags for electronic article surveillance tags*. IEEE Transactions on Advanced Packaging, 2009. **32**(1): p. 72-76.
17. Suganuma K., *Introduction to Printed Electronics (Book)*. Springer Briefs in Electrical and Computer Engineering, 2014. Springer Science + Business Media, New York Springer. p. 1-124.
18. Jayasiri H. B., Purushothaman C. S. and Vennila A., *Quantitative analysis of plastic debris on recreational beaches in Mumbai, India*. Marien Pollution Bulletin, 2013. **77**: p. 107-122.
19. Thamae T., Bailie C., *Natural fiber composites: turning waste into useful materials*. VDM Publishing, 2009. p. 1-7.
20. Willför S., et al., *Characterization of water-soluble galactoglucomannans from Norway spruce wood and thermomechanical pulp*. Carbohydrate Polymers, 2003. **52**: p. 175-187.
21. Song T., (2008) *Extraction of galactoglucomannan from spruce wood with pressurized hot water*. Holzforschung 2008. **62**: p. 659-666.
22. Kisonen V., et al., *Cationised O-acetyl galactoglucomannans: synthesis and characterisation*. Carbohydrate Polymer, 2014. **99**: p. 755-764.
23. Mikkonen K. S., *Crosslinking with ammonium zirconium carbonate improves the formation and properties of spruce galactoglucomannan films*. Journal of Material Science, 2013. **48**: p. 4205-4213.
24. Lozhechnikova A, et al., *Modification of nanofibrillated cellulose using amphiphilic block-structured galactoglucomannans*. Carbohydrate Polymer, 2014. **110**: p. 163-172.
25. Mikkonen K. S., Stevanic J. S., Joly C., et al., *Composite films from spruce galactoglucomannans with microfibrillated spruce wood cellulose*. Cellulose, 2011. **18**: p. 713-726.
26. Trovatti E., et al., *Nano-fibrillated cellulose composite films with improved thermal and mechanical properties*. Composite Science Technology, 2012. **72**: p. 1556-1561

27. Escalante A., et al., (2012) *Flexible oxygen barrier films from spruce xylan*. Carbohydrate Polymer, 2012. **87**: p. 2381-2387.
28. Isogai A., *Wood nano-celluloses: fundamentals and applications as new bio-based nanomaterials*. Journal of Wood Science, 2013. **59**: p. 449-459.
29. Paäkkö, M., et al., *Enzymatic hydrolysis combined with mechanical shearing and high-pressure homogenization for nanoscale cellulose fibrils and strong gels*. Biomacromolecules, 2007. **8** (6): p. 1934-1941.
30. Petersen, K., et al., *Potential of bio-based materials for food packaging*. Trends in Food Science and Technology, 1999. **10** (3): p. 52-68.
31. Henriksson, M., et al., *Cellulose nanopaper structures of high toughness*. Biomacromolecules, 2008. **9** (6) 1579-1585.
32. Lavoine, N., et al., *Microfibrillated cellulose - its barrier properties and applications in cellulosic materials: a review*. Journal of Carbohydrate Polymer, 2012., **90** (2): p. 735-764.
33. Spence, K. L., et al., *The effect of chemical composition on microfibrillar cellulose films from wood pulps: Water interactions and physical properties for packaging applications*. Cellulose, 2010. **17** (4): p. 835-848.
34. Rodionova, G., et al., *Surface chemical modification of microfibrillated cellulose: Improvement of barrier properties for packaging applications*. Cellulose, 2011. **18**: p. 127-134.
35. Syverud K. and Stenius P., *Strength and barrier properties of MFC films*. Cellulose, 2009. **16**: p. 75-85.
36. Okuba K., Fujii T. and Yamashita N., *Improvement of interfacial adhesion in bamboo polymer composite enhanced with microfibrillated cellulose*. JSME International Journal of Series A: Solid Mechanics and Materials Engineering, 2005. **48**: p. 199-204
37. Zhang Z., et al., *Ultra-lightweight and flexible silylated nano-fibrillated cellulose sponges for the selective removal of oil from water*. Chemistry of Materials, 2014. **26**: p. 2659-2668.
38. Vuoti S., Talja R., Johansson L. S., et al., *Solvent impact on esterification and film formation ability of nanofibrillated cellulose*. Cellulose, 2013. **20**: p. 2359-2370.

39. Besbes I, Vilar M. R., Boufi S., *Nanofibrillated cellulose from alfa, eucalyptus and pine fibres: preparation, characteristics and reinforcing potential*. Carbohydrate Polymer, 2011. **86**: p. 1198-1206.
40. Österberg M., et al., *A fast method to produce strong NFC films as a platform for barrier and functional materials*. ACS Applied Materials and Interfaces, 2013. **5**: p. 4640-4647.
41. Medoff, Marshall et al., *Cellulosic and lignocellulosic materials and compositions and composites made therefrom*. July 2006, US Patent 7,074,918;
42. Tucker, Jr., et al., *Flexible microwave cooking pouch containing a raw frozen protein portion and method of making*, March 2006, US Patent 2801930A.
43. Lin Li, *Global environmental packaging requirements*, Barrier Coating Symposium, Western Michigan University, Oct. 12-13, 2004, Kalamazoo, MI.
44. Akkapeddi, Murali K. et al., *Oxygen scavenging high barrier polyamide compositions for packaging applications*. US Patent, 2004. Patent number 6,740,698.
45. Deborah L., et al., *All starch nanocomposite coating for barrier material*. Journal of Applied Polymer Science, 2014. **131**:39826
46. Michael M., et al., *UV-cured, flexible, and transparent nanocomposite coating with remarkable oxygen barrier*. Advanced Materials, 2012. **24**: p. 2142-2147.
47. Foster J., et al., *Dispersion and phase separation of carbon nanotubes in ultra-thin polymer films*. Journal of Colloid and Interface Science, 2005. **287**, p. 167-172.
48. Beall G. and Pinnavaia J., *Polymer-clay nanocomposites (Book)*, Wiley series in Polymer Science Jan. 2001. P. 231-235
49. Kanatt, S. R., Rao, M. S., Chawla, S. P., and Sharma, A., *Active chitosan-polyvinyl alcohol films with natural extracts*. Food Hydrocolloids, 2012. **29**(2): p. 290-297.
50. Hansen, N. M. L., & Plackett, D., *Sustainable films and coatings from hemicelluloses: A review*. Biomacromolecules, 2008. **9**(6): p. 1493-1505
51. Goksu, E. I., Karamanlioglu, M., Bakir, U., Yilmaz, L., and Yilmazer, U., *Production and characterization of films from cotton stalk xylan*. Journal of Agricultural and Food Chemistry, 2007. **55**(26): p. 10685-10691.

52. Gröndahl, M., Eriksson, L. and Gatenholm, P., *Material properties of plasticized hardwood xylans for potential application as oxygen barrier films*. Biomacromolecules, 2004. **5**(4): p. 1528-1535.
53. Peng, X. W., Ren, J. L., Zhong, L. X. and Sun, R. C., *Nanocomposite films based on xylan-rich hemicelluloses and cellulose nanofibers with enhanced mechanical properties*. Biomacromolecules, 2011. **12**(9), 3321-3329.
54. Ma, X. F., Chang, P. R., Yu, J. G. and Stumborg, M., *Properties of biodegradable citric acid-modified granular starch/thermoplastic pea starch composites*. Carbohydrate Polymers, 2009. **75**(1): p. 1-8.
55. Reddy, N. and Yang, Y. Q., *Citric acid cross-linking of starch films*. Food Chemistry, 2010. **118**(3): p. 702-711.
56. Shi, R., et al., *The effect of citric acid on the structural properties and cytotoxicity of the polyvinyl alcohol/starch films when molding at high temperature*. Carbohydrate Polymers, 2008. **74**(4), p. 763-770.
57. Perelaer J., et al., *Printed electronics: the challenges involved in printing devices, interconnects, and contacts based on inorganic materials*. Journal of Materials Chemistry, 2010. **20**: p.8446-8453.
58. Peng C. Y., et al., *Flexible CZTS Solar Cells on Flexible Corning Willow Glass Substrates*. Photovoltaic Specialist Conference, 2014. Denver, CO: IEEE.
59. Nogi M., et al., *Optically transparent nanofiber paper*. Advanced Materials, 2009. **21** (16): p.1595-1598.
60. Jiu J., et al., *Strongly adhesive and flexible transparent silver nanowire conductive film fabricated with high-intensity pulsed light technique*. Journal of Materials Chemistry, 2012. **22**: p.23561-23567.
61. Suganuma, K., *Introduction to Printed Electronics(Book)*. Springer Briefs in Electrical and Computer Engineering. 2014, Springer Science+Business Media New York Springer. p. 220-235.
62. T. Young, *An essay on the cohesion of fluids*. Philosophical Transactions, Royal. Society Publishing, 1805. **95**: 65-87.

63. Adamson, W. and Gast, A.P., *Physical chemistry of surface (Book)*, Wiley Publishing, 1997. p.235-250.
64. Precision tensiometers <http://www.attension.com/> Date accessed: July 7, 2018
65. Owens, D. K. and Wendt, R. C., *Estimation of the surface free energy of polymers*. Journal of Applied Polymer Science, 1969. **13**(8): p. 1741-1747.
66. Pomerantz P., Clinton W. C., and Zisman W. A., *Spreading pressures and coefficients, interfacial tensions, and adhesion energies of the lower alkanes, alkenes, and alkyl benzenes on water*. Journal of Colloid Interface Science, 1967. **24**(1): p.16-28.
67. M. P. Michael and M. Darianian, *Architectural solutions for mobile RFID services for the internet of things*. Proceedings of. IEEE Congress on Services Part 1, 2008. p. 71–74.
68. G. Kortuem, F. Kawsar, D. Fitton, and V. Sundramoorthy, *Smart objects as building blocks for the internet for things*. IEEE Internet Computing, 2010. **14**(1): p. 44-51.
69. Alastalo A., et al., *Printed WORM memory on a flexible substrate based on rapid electrical sintering of nanoparticles*. IEEE Transactions on Electron Devices, 2011. **58**(1): p. 151-159.
70. Kang J., Kim R. H. and Hahn H., *Sintering of inkjet-printed silver nanoparticles at room temperature using intense pulsed light*. Journal of Electronic Materials, 2011. **40**(11): p. 2268-2277.
71. Pacquit J., *Development of a smart packaging for the monitoring of fish spoilage*. Food Chemistry, 2007. **102**(2): p. 466-470.
72. Subramanian V., et al., *Printed electronics for low-cost electronic systems: Technology status and application development*. Proceedings of 38th European Solid State Device Research Conference (ESSDERC), 2008. p. 17-24.
73. Tan E. L., et al., *A wireless, passive sensor for quantifying packaged food quality*. Sensors, 20047. **7**(9): p. 1747-1756.
74. Harpster T.J., Stark B., and Najafi K., *A passive wireless integrated humidity sensor*. Sensors and Actuators A: Physical, 2002. **95**(2): p. 100-107.
75. A. S. G. Reddy, B. B. Narakathu, M. Z. Atashbar, M. Rebros, E. Rebrosova, M. Joyce, B. J Bazuin, P. D. Fleming, A. Pekarovicova, “Printed capacitive based humidity sensors on flexible substrates”, Sensors Letters, vol. 9 pp. 869-871, 2011.

76. Tomas Unander and Hans-Erik Nilsson, *Characterization of printed moisture sensors in packaging surveillance applications*. IEEE Sensors Journal, 2009. **9** (8): p. 922-928.
77. Juho A.S., et al., *Biocomposite cellulose-alginate films: Promising packaging materials*. Food Chemistry, 2014. **151**: p. 343-351.
78. Vuoti S., et al., *Chemical modification of cellulosic fibers for better convertibility in packaging applications*. Cellulose, 2013. **96**(2): p. 549-559.
79. Stevanic J.S., et al., *Arabinoxylan/nanofibrillated cellulose composite films*. Journal of Material Science, 2012. **47**(18): 6724-6732.
80. Saxena A., Elder T. and Ragauskas A.J., *Moisture barrier properties of xylan composite films*. Carbohydrate Polymer, 2011. **84**(4): p. 1371-1377.
81. Kayserilioglu, B.S., et al., *Use of xylan, an agricultural by-product, in wheat gluten based biodegradable films: mechanical, solubility and water vapor transfer rate properties*. Bioresource Technology, 2003. **87**(3): p. 239-246.
82. Abdul Khalil, H. P. S., Bhat, A. H., & Ireana Yusra, A. F., *Carbonhydr. Polym.*, **87**, 963, (2012).
83. Oinonen P., Areskog D., Henriksson G., "The processing and upgrading of hemicellulose mixtures", 16th International Symposium on Wood, Fiber, and Pulp Chemistry, ISWFPC, 2011, pp 1028-1031.
84. Egues I., Eceiza A. and Labidi J., *Effect of different hemicelluloses characteristics on film forming properties*. Industrial Crops Products, 2013. **47**: p. 331-338.
85. Lu Z. X., et al., *Arabinoxylan fiber, a byproduct of wheat flour processing, reduces the postprandial glucose response in normoglycemic subjects*. The American Journal of Clinical Nutrition, 2000. **71**(5): p. 1123-1128.
86. Pekarovic J., Busso M., Raycraft L., and Pekarovicova A., *Bioenergy and Value-added Products from Switchgrass*. 3rd International Scientific Conference, Slovakia, 2012. p. 108-112.
87. Sjostrom E., *Wood Chemistry (Book) 2nd Ed*. Academic Press, San Diego, 1993.
88. Ruiz H., et al., *Biorefinery valorization of autohydrolysis wheat straw hemicellulose to be applied in a polymer-blend film*. Carbohydrate Polymer, 2013. **92**(2): p. 2154-2162.
89. Blazej A., Kosik M., *Fytomasa ako chemicka surovina*, edited by Veda, Slovak Academy of

- Science, Bratislava, 1985.
90. Saito T., Kuramae R., Wohler J., Berglund L. and Isogai A., *An ultrastrong nanofibrillar biomaterial: the strength of single cellulose nanofibrils revealed via sonication-induced fragmentation*. Biomacromolecules, 2013. **14**(1): p. 248-253.
 91. Ragauskas, A. J., et al., *The path forward for biofuels and biomaterials*. Science, 2006. **311**(5760): p. 484-489.
 92. Sun. R. C., Sun, X. F. and Tomkinson J., *Hemicellulose: Science and Technology*, edited by Gatenholm, P., Tenkanen. American Chemical Society, 2004. p. 2-22.
 93. Ebringerova, A., *Structural diversity and application potential of hemicelluloses*. Macromolecular Symposia, 2006. **232**(1): p. 1-12.
 94. Ebringerova, A.; Hroomadkova, Z. and Heinze, T., *Hemicellulose*. Advanced Polymer Science, 2005. **186**(1): p. 1-68
 95. Lindblad, M. S., Albertsson, A. C., in "Polysaccharides: Structural diversity and functional versatility", edited by Dumitriu, S., Ed., Marcel Dekker: New York, 2005, pp. 491-508.
 96. Sun, X. F., et al., *Characteristics of degraded cellulose obtained from steam-exploded wheat straw*. Carbohydrate Research, 2005. **340**(1): p. 97-106.
 97. Grondahl, M., Eriksson, L. and Gatenholm, P., *Material properties of plasticized hardwood xylans for potential application as oxygen barrier films*. Biomacromolecules, 2004. **5**(4): p. 1528-1535.
 98. Lai, V. M. F., Lu, S., He, W. H. and Chen, H. H., *Non-starch polysaccharide compositions of rice grains with respect to rice variety and degree of milling*. Food Chemistry, 2006. **101**: p. 1205-1210.
 99. Smart, C. L. and Whistler, R. L., *Films from hemicellulose Acetates*. Science, 1949. **110**(2870): p. 713-714.
 100. Hansen N.M. and Plackett D., *Sustainable films and coatings from hemicelluloses: A review*. Biomacromolecules, 2008. **9**(6): p. 1493-1505.
 101. Ten, E. and Vermerris, W., *Functionalized polymers from lignocellulosic biomass: state of the art*. Polymers, 2013. **5**: p. 600-642.
 102. Arola S., Malho J. M., Laaksonen P., et al., *The role of hemicellulose in nano-fibrillated cellulose networks*. Soft Matter, 2013. **9**(4): p. 1319-1326.

103. Darcy, H., *Les Fontaines Publiques de la Ville de Dijon*, Dalmont, Paris, 1856.
104. Douglas C. Montgomery, *Design and Analysis of Experiment (Book)*. John Wiley & Sons, Inc., 2005. p. 203-254.
105. H. E. Messmer Ltd., *Operating and Maintenance Instructions for the Parker Print-Surf Roughness and Porosity Tester*. H. E. Messmer Ltd., Britain, 2005.
106. Lokendra Pal, Margaret K. Joyce and P. D. Fleming, *A simple method for calculation of permeability coefficient of porous media*. TAPPI Journal, 2006. p. 10.
107. Othman, S. H., *Bio-nanocomposite materials for food packaging applications: types of bio polymer and nano-sized filler*. Agriculture and Agricultural Science Procedia, 2014. **2**: p. 296-303.
108. BCC Research. (2014). *Global markets and technologies for bioplastics*. Report code PLS050C. Available at <http://www.bccresearch.com/market-research/plastics/bioplastics-pls050c.html> Accessed 17.06.18.
109. Helmut Kaiser Consultancy, 2013. *Bioplastics market worldwide 2010/11-2015- 2020-2025*. Available at <http://www.hkc22.com/bioplastics.html>. Accessed 09.07.18.
110. Giancone, T., Torrieri, E., Di Pierro, P., et al., *Effect of surface density on the engineering properties of high methoxyl pectin-based edible films*. Food and Bioprocess Technology, 2011. **4**: p. 1228-1236.
111. Janjarasskul, T. and Krochta, J. M., *Edible packaging materials*. Annual Reviews of Food Science and Technology, 2010. **1**: p. 415-448.
112. Sebti, I., Delves-Broughton, J. and Coma, V., *Physicochemical properties and bioactivity of nisin-containing cross-linked hydroxypropylmethylcellulose films*. Journal of Agricultural and Food Chemistry, 2003. **51**: p. 6468-6474.
113. Balaguer, M. P., Gomez-Estaca J., Gavara, R. and Hernandez-Munoz, P., *Functional properties of bio-plastics made from wheat gliadins modified with cinnamaldehyde*. Journal of Agricultural and Food Chemistry, 2011. **59**: p. 6689-6695.
114. Ma, R., Pekarovicova, A., Fleming, P. D. and Husovska, V., *Preparation and characterization of hemicellulose-based printable films*. Cellulose chemistry and Technology, 2017. **49** (7): p. 2879-2893

115. Forssell, P., Lahtinen, R., Lahelin, M. and Myllärinen, P. *Oxygen permeability of amylose and amylopectin films*. Carbohydrate Polymers, 2002. **47**: p. 125-129.
116. Godbillot, L., Dole, P., Joly, C., Rogé, B. and Mathlouthi, M., *Analysis of water binding in starch plasticized films*. Food Chemistry, 2006. **96**, p. 380-386.
117. Stading, M., Rindlav-Westling, Å. and Gatenholm, P., *Humidity-induced structural transitions in amylose and amylopectin films*. Carbohydrate Polymers, 2001. **45**: p. 209-217.
118. Gatenholm, P., Bodin, A., Grondahl, M., et al., *Polymeric film or coating comprising hemicellulose*. Patent US 7,427,643 B2. September 2008.
119. Grondahl, M., et al., *Polymeric film or coating comprising hemicellulose*. 2013. U.S. Patent, 8,557,033.
120. Eriksen, Ö., Syverud, K., and Gregerson, Ö., *The use of microfibrillated cellulose produced from kraft pulp as strength enhancer in TMP paper*. Nordic Pulp and Paper Research Journal, 2008. **23**(3): p. 299-304.
121. Syverud, K., Gregersen, O., Chinga-Carrasco, G. and Eriksen, O., *The influence of microfibrillated cellulose, MFC, on paper strength and surface properties*. Proceedings of Advances in Pulp and Paper Research Symposium, 2009. Oxford, UK, p. 899-930.
122. Syverud, K. and Stenius, P., *Strength and barrier properties of MFC films*. Cellulose, 2009. **16**(1), p. 75-85.
123. Aulin, C., Gallstedt, M., and Lindström, T., *Oxygen and oil barrier properties of microfibrillated cellulose films and coatings*. Cellulose, 2010a. **17**(3), p. 559-574.
124. Ridgway, C. J., and Gane P. A. C., *Constructing NFC-pigment composite surface treatment for enhanced paper stiffness and surface properties*. Cellulose 2012. **19**(2), p. 547-560.
125. Lavoine, N., Bras, J. and Desloges, I., *Mechanical and barrier properties of cardboard and 3D packaging coated with microfibrillated cellulose*. Journal of Applied Polymer Science, 2014a. **131**(8), article number. 40106.
126. Tammelin, T., Hippi, U., Salminen, A., and Salminen, T., *Preparing a film of nanofibrillated cellulose on surface of support material, which is useful for producing e.g. food packaging material, comprises applying and spreading suspension of cellulose onto plastic support material,*” US Patent, 2013. US2014255688-A1.

127. Vartiainen, J., Shen, Y. F., Kaljunen, T., et al., *Bio-based multilayer barrier films by extrusion, dispersion coating and atomic layer deposition*. Journal of Applied Polymer Science, 2015. **133**(2): article number 42260.
128. Aulin, C., Johansson, E., Wågberg, L. and Lindström, T., *Self-organized films from cellulose nanofibrils using the layer-by-layer technique*. Biomacromolecules, 2010b. **11**(4): p. 872-882.
129. Rodionova, G., Lenes, M., Eriksen, O. and Gregersen, O., *Surface chemical modification of microfibrillated cellulose: Improvement of barrier properties for packaging applications*. Cellulose, 2011. **18**(1): p. 127-134.
130. Aulin, C., Karabulut, E., Tran, A., Wågberg, L. and Lindström, T., *Transparent nanocellulosic multilayer thin films on polylactic acid with tunable gas barrier properties*. ACS Applied Materials Interfaces, 2013. **5**(15): p. 7352-7359.
131. Kumar, V., Bollstrom, R., Yang, A., Chen, Q. X., et al., *Comparison of nano- and microfibrillated cellulose films*. Cellulose, 2014. **21**(5), p. 3443-3456.
132. Honorato, C., Kumar, V., Liu, J., Koivula, H., Xu, C. L. and Toivakka, M., *Transparent nano-fibrillated cellulose-pigment composite films*. Journal of Material Science, 2015. **50**(22), 7343- 7352.
133. Ma, X., et al., *Properties of biodegradable citric acid-modified granular starch/thermoplastic pea starch composites*. Carbohydrate Polymers, 2009. **75**(1): p. 1-8.
134. Coma, V., Sebti, I., Pardon, P., Pichavant, F. H. and Deschamps, A., *Film properties from crosslinking of cellulosic derivatives with a poly-functional carboxylic acid*. Carbohydrate Polymers, 2003. **51**, p. 265-271.
135. Olsson, E., et al., *The effect of pH on hydrolysis, crosslinking and barrier properties of starch barriers containing citric acid*. Carbohydrate Polymers, 2013. **98**(2): p. 1505-1513.
136. Herrera, M.A., Matthew, A. P., and Oksman, K., *Barrier and mechanical properties of plasticized and cross-linked nano-fibrillated cellulose coatings for paper packaging applications*. Cellulose, 2017. **24** (9), p. 3969-3980.
137. American Society for Testing and Materials. (1993). Standard test methods for water vapor transmission of material. E96, Annual book of ASTM standards.
138. Khalifa, Y. I. M., *Effect of the printing remedies and lamination techniques on barrier*

- properties “WVTR and OTR value” for polypropylene film.* EC Nutrition, 2016. **5**(2): p. 1089-1099
139. Girifalco, L.A., and Good, R.J., *A theory for the estimation of surface and interfacial energies. I. Derivation and application to interfacial tension.* Journal of Physical Chemistry, 1957. **61**(7): p. 904-909.
 140. Abdillahi, H., et al., *Influence of citric acid on thermoplastic wheat flour/poly (lactic acid) blends. II. Barrier properties and water vapor sorption isotherms.* Industrial Crops and Products, 2013. **50**: p. 104-111.
 141. Wang, S., et al., *Properties of polyvinyl alcohol/xylan composite films with citric acid.* Carbohydrate Polymers, 2014. **103**: p. 94-99.
 142. Zou, G. X., Qu, J. P., and Zou, X. L., *Optimization of water absorption of starch/PVA composites.* Polymer Composites, 2007. **28**(5): p. 674-679.
 143. Zhang W, Xiao H and Qian L., *Enhanced water vapor barrier and grease resistance of paper bilayer-coated with chitosan and beeswax.* Carbohydrate Polymers, 2014. **101**: p. 401- 406.
 144. Bordenave N, Grelier S and Coma V., *Hydrophobization and Antimicrobial Activity of Chitosan and Paper-based Packaging Material.* Biomacromolecules, 2010. **11**: p. 88-96.
 145. M., Tuomas Mehtio et al., *Crosslinkable poly (lactic acid)-based materials: Biomass-derived solution for barrier coatings.* Journal of Applied Polymer Science, 2016. **134**: 44326.
 146. Mathew A, Thielemans W and Dufresne A., *Mechanical properties of nanocomposites from sorbitol plasticized starch and tunicin whiskers.* Journal of Applied Polymer Science, 2008. **109**: p. 4065-4074.
 147. Xiao C, et al., *Properties of regenerated cellulose films plasticized with α -monoglycerides.* Journal of Applied Polymer Science, 2003. **89**: p. 3500-3505.
 148. Hansen N, Blomfeldt T, Hedenqvist M, Plackett D., *Properties of plasticized composite films prepared from nanofibrillated cellulose and birch wood xylan.* Cellulose, 2012. **19**: p. 2015-2031
 149. Liu X, et al., *Regenerated cellulose film with enhanced tensile strength prepared with ionic liquid 1-ethyl-3-methylimidazolium acetate (EMI- MAc).* Cellulose, 2013. **20**:1391-1399.

150. Wang S., et al., *Choline Chloride/urea as an effective plasticizer for production of cellulose films*. Carbohydrate Polymer, 2015. **117**: p. 133-139.
151. De Cuadro P., et al., *Crosslinking of cellulose and poly (- ethylene glycol) with citric acid*. Reactive and Functional Polymers, 2015. **90**: p. 21-24.
152. Matsumura H., Sugiyama J. and Wolfgang G., *Cellulosic nanocomposites. I. Thermally deformable cellulosic hexanoates from heterogeneous reaction*. Journal of Applied Polymer Science, 2000. **78**:2242-2253.
153. Vuoti S., et al., *Solvent impact on esterification and film formation ability of nanofibrillated cellulose*. Cellulose, 2013. **20**: p. 2359-2370.
154. Quellmalz A., and Mihranyan A., *Citric acid crosslinked nano-fibrillated cellulose-based paper for size-exclusion nanofiltration*. ACS Biomaterials Science and Engineering, 2015.**1**: p. 271-276.
155. Zhou Y J., Luner P. and Caluwe P., *Mechanism of cross-linking of paper with polyfunctional carboxylic acids*. Journal of Applied Polymer Science, 1995. **58**: p. 1523-1534.
156. Sirvio J., et al., *Biocomposite cellulose-alginate films: promising packaging materials*. Food Chemistry, 2014. **151**: p. 343-351.
157. Ma R., Pekarovicova, A., Fleming, P. D., *Biopolymer Films from Glucomannan: The effects of Citric Acid Crosslinking on Barrier Properties*. Journal of Print Media Technology Research, 2018. 1 (7): p. 19-25.
158. Mäkelä, T., et al., *Continuous roll-to-roll nanoimprinting of inherently conducting polyaniline*. Microelectronic Engineering, 2007. 84 (5-8): p. 877-879.
159. Kololuoma T. K., et al., *Towards roll-to-roll fabrication of electronics, optics, and optoelectronics for smart and intelligent packaging*. Proceedings of the SPIE 5363, Emerging Optoelectronic Applications, 2004. p. 77.
160. Danick B., et al., *Making environmental sensors on plastic foil*. Materials Today, 2011. **14** (9): p. 416-423.
161. Lee CY., et al., *Fabrication of micro sensors on a flexible substrate*. Sensors and Actuators A: Physical, 2008. **147** (1): p. 173-176.

162. Zampetti E., et al., *Design and optimization of an ultra thin flexible capacitive humidity sensor*. Sensors and Actuators B: Chemical, 2009. **143** (1): p. 302-307.
163. Traversa, E. et al., *Environmental Monitoring Field Tests Using Screen-Printed Thick-Film Sensors Based on Semiconducting Oxides*. Sensors and Actuators B: Chemical, 2000. **65**: p. 181-185.
164. Kunte, G. V.; Shivashankar, S.A. and Umarji, A. M., *Humidity Sensing Characteristics of Hydrotungstite Thin Films*. Bulletin of Material Science, 2009. **31**: p. 835-839.
165. Mamishev, A. V., Sundara-Rajan, K. and Zahn, M., *Interdigital Sensors and Transducers*. Proceedings of IEEE, 2004. **92**: p. 808-845.
166. Moneyron, J. E., de Roy, A. and Besse, J.P., *Realisation of a Humidity Sensor Based on the Protonic Conductor $Zn_2Al(OH)_6Cl_nH_2O$* . Microelectronics International, 1991. **8**: p. 26-31.
167. Kim, E. et al., *Colorimetric and Resistive Polymer Electrolyte Thin Films for Real-Time Humidity Sensors*. ACS Applied Materials & Interfaces, 2012. **4**: p. 5179-5187.
168. Wang, W. et al., *Humidity Sensor Based on LiCl-Doped ZnO Electrospun Nanofibers*. Sensors and Actuators B: Chemical, 2009. **141**: p. 404-409.
169. Anbia, M. et al., *Humidity Sensing Properties of the Sensor Based on V-Doped Nanoporous $Ti_{0.9}Sn_{0.1}O_2$ Thin Film*. Chinese Journal of Chemistry, 2012. **30**: p. 842-846.
170. Hamid F., et al., *Humidity sensors principle, mechanism and fabrication technologies: a comprehensive review*. Sensors, 2014. **14** (5): p. 7881-7939.
171. Li Y., et al., *Monolithic CMOS multi-transducer gas sensor microsystem for organic and inorganic analytes*, Sensors and Actuators B: Chemical, 2007. **126** (2): p. 431-440.
172. Turkani S. V., et al, *A carbon nanotube based NTC thermistor using additive print manufacturing processes*. Sensors and Actuators A: Physical, 2018. **279**: p.1-9.

LIST OF PUBLICATIONS

Peer Reviewed Publications

- Publication I.** Ma R., Pekarovicova, A., Fleming, P. D., *Biopolymer Films from Glucomannan: The effects of Citric Acid Crosslinking on Barrier Properties*. Journal of Print and Media Research Technology, 2018. 7 (1), p. 19-25.
- Publication II.** Ma R., Pekarovicova, A., Fleming, P. D., *The preparation and characterization of hemicellulose-based printable films*. Cellulose Chemistry and Technology, 2017. 51(9-10), p. 939-948.
- Publication III.** Ma R., Pekarovicova, A., Fleming, P. D., *Screen printed moisture sensor on hemicellulose based barrier coated SBS board*. Journal of Print and Media Research Technology (in preparation).
- Publication IV.** Ma R., Wang Y., Cao C., Xia W., *The formulation of silver doped lanthanum titanate photochromic ink and its application*. Journal of Xi'an University of Technology, 2014. 30 (4), p. 15-18.

Conference Proceedings

1. Ma R., Pekarovicova, A., Fleming, P. D., *The hemicellulose-based barrier coating formulations and characterizations*. Proceedings of the 2017 TAGA Technical Association of the Graphic Arts, March 2017, p. 36-41.
2. Ma R., Pekarovicova, A., Fleming, P. D., *Hemicellulose-based Barrier Coating for Packaging*. Research and Creative Activities Poster Day. 236 http://scholarworks.wmich.edu/grad_research_posters/236/
3. Ma R., Pekarovicova, A., Fleming, P. D., *The hemicellulose-based printable films*. Proceedings of the 2016 TAGA Technical Association of the Graphic Arts, March 2016, pp. 125-130.

Presentations

1. “*The Hemicellulose-based Barrier Coatings for Packaging*”, TAGA 69th, Houston, Texas, March 19-22, 2017. <http://tagaatc.printing.org/authors/ruoxi-ma/>
2. “*The Formulation and Characterizations of Cross-linking Hemicellulose-based Barrier*

Coating for Packaging”, TAPPI’s PaperCon 10th, Minneapolis, Minnesota, April 23-25, 2017.

3. *“Hemicellulose-based Barrier Coating for Packaging”*, Research and Creative Activities Poster Day, Western Michigan University, Kalamazoo, Michigan, April 13, 2017.
4. *“The Development of Biodegradable Materials and Printable Substrates for Food Packaging”*, Flexo Day at Western Michigan University, April 20, 2017.

“Hemicellulose-based printable films”, TAGA 68th, Memphis, Tennessee, March 20-23, 2016.